Self-incompatibility-induced programmed cell death in field poppy pollen involves dramatic acidification of the incompatible pollen tube cytosol

Wilkins, Katie A.; Bosch, Maurice; Haque, Tamanna; Teng, Nianjun; Poulter, Natalie S.; Franklin-tong, Vernonica E.

DOI:
10.1104/pp.114.252742

License:
Other (please specify with Rights Statement)

Document Version
Publisher's PDF, also known as Version of record

Citation for published version (Harvard):
Wilkins, KA, Bosch, M, Haque, T, Teng, N, Poulter, NS & Franklin-tong, VE 2015, 'Self-incompatibility-induced programmed cell death in field poppy pollen involves dramatic acidification of the incompatible pollen tube cytosol', *Plant Physiology*, vol. 167, no. 3, pp. 766-779. https://doi.org/10.1104/pp.114.252742

Self-Incompatibility-Induced Programmed Cell Death in Field Poppy Pollen Involves Dramatic Acidification of the Incompatible Pollen Tube Cytosol[1][OPEN]

Katie A. Wilkins[2], Maurice Bosch[3], Tamanna Haque, Nianjun Teng[4], Natalie S. Poulter[5], and Vernonica E. Franklin-Tong*

School of Biosciences, University of Birmingham, Edgbaston, Birmingham B15 2TT, United Kingdom

Self-incompatibility (SI) is an important genetically controlled mechanism to prevent inbreeding in higher plants. SI involves highly specific interactions during pollination, resulting in the rejection of incompatible (self) pollen. Programmed cell death (PCD) is an important mechanism for destroying cells in a precisely regulated manner. SI in field poppy (*Papaver rhoeas*) triggers PCD in incompatible pollen. During SI-induced PCD, we previously observed a major acidification of the pollen cytosol. Here, we present measurements of temporal alterations in cytosolic pH ($[pH]_{cyt}$); they were surprisingly rapid, reaching pH 6.4 within 10 min of SI induction and stabilizing by 60 min at pH 5.5. By manipulating the $[pH]_{cyt}$ of the pollen tubes in vivo, we show that $[pH]_{cyt}$ acidification is an integral and essential event for SI-induced PCD. Here, we provide evidence showing the physiological relevance of the cytosolic acidification and identify key targets of this major physiological alteration. A small drop in $[pH]_{cyt}$ inhibits the activity of a soluble inorganic pyrophosphatase required for pollen tube growth. We also show that $[pH]_{cyt}$ acidification is necessary and sufficient for triggering several key hallmark features of the SI PCD signaling pathway, notably activation of a DEVDase/caspase-3-like activity and formation of SI-induced punctate actin foci. Importantly, the actin binding proteins Cyclase-Associated Protein and Actin-Depolymerizing Factor are identified as key downstream targets. Thus, we have shown the biological relevance of an extreme but physiologically relevant alteration in $[pH]_{cyt}$ and its effect on several components in the context of SI-induced events and PCD.

Programmed cell death (PCD) in plants is relatively well documented and characterized (Jones and Dangl, 1996; van Doorn, 2011; van Doorn et al., 2011). There is considerable biochemical evidence for the involvement of caspase-like activities in plant PCD (van Doorn and Woltering, 2005). For example, the vacuolar processing enzyme has YVADase (caspase-1-like) activity (Hatsugai et al., 2004; Rojo et al., 2004; Hara-Nishimura et al., 2005), DEVDase (caspase-3-like) and YVADases are associated with PCD in several plant systems (del Pozo and Lam, 1998; Korthout et al., 2000; Danon et al., 2004), and VEIDase (caspase-6-like) is the main caspase-like activity involved in embryonic pattern formation (Bozhkov et al., 2004). However, because plants have no caspase gene homologs (Sanmartín et al., 2005), the nature of their caspase-like enzymes is the subject of considerable debate. Vacuolar cell death is one of two major classes of PCD in plants (van Doorn et al., 2011). It is thought that collapse of the vacuole is a key irreversible step in several plant PCD systems, including during tissue and organ formation, such as the classic differentiation of tracheary elements (Hara-Nishimura and Hatsugai, 2011). Exactly how this is achieved and what processes are involved remain unknown. Until very recently, it was generally thought that the rupturing vacuole releases proteases, hydrolases, and nucleases, allowing cellular disassembly by an autophagy-like process. Some PCD systems cannot be assigned to either class; these include PCD triggered by the hypersensitive response to biotrophic pathogens, PCD in cereal endosperm, and self-incompatibility (SI)-induced PCD (van Doorn et al., 2011).

SI is a genetically controlled pollen-pistil cell-cell recognition system. Self-pollen is recognized by the stigma as being genetically identical, resulting in inhibition of pollen tube growth. Most SI systems use tightly linked polymorphic genes: the pollen (male) and pistil (female) *S*-determinants. In field poppy (*Papaver rhoeas*), the *S*-determinants are a 14-kD signaling ligand field poppy stigma S (PrsS) and a unique transmembrane protein field poppy pollen S (PrpS; Foote et al., 1994; Wheeler et al., 2010). These interact in an *S*-specific manner, and

[1] This work was supported by the Biotechnology and Biological Sciences Research Council (PhD studentship to K.A.W. and funding to the laboratory of V.E.F.-T.) and the China Scholarship Council (to N.T.).

[2] Present address: Department of Plant Sciences, University of Cambridge, Cambridge CB2 3EA, UK.

[3] Present address: Institute of Biological, Environmental and Rural Sciences, Aberystwyth University, Gogerddan, Aberystwyth SY23 3EB, UK.

[4] Present address: College of Horticulture, Nanjing Agricultural University, Nanjing 210095, China.

[5] Present address: Institute of Biomedical Research, University of Birmingham, Edgbaston, Birmingham B15 2TT, UK.

* Address correspondence to V.E.Franklin-Tong@bham.ac.uk.

The author responsible for distribution of materials integral to the findings presented in this article in accordance with the policy described in the Instructions for Authors (www.plantphysiol.org) is: Vernonica E. Franklin-Tong (v.e.franklin-tong@bham.ac.uk).

[OPEN] Articles can be viewed without a subscription.

www.plantphysiol.org/cgi/doi/10.1104/pp.114.252742

increases in cytosolic free calcium ($[Ca^{2+}]_{cyt}$) are triggered in incompatible pollen tubes (Franklin-Tong et al., 1993), resulting in phosphorylation of soluble inorganic pyrophosphatases (sPPases; Rudd et al., 1996; de Graaf et al., 2006), activation of a Mitogen-Activated Protein Kinase (MAPK; Rudd et al., 2003), and increases in reactive oxygen species (ROS) and nitric oxide (Wilkins et al., 2011, 2014). Most of these components are integrated into a signaling network leading to PCD (Bosch et al., 2008; Wilkins et al., 2014). The actin cytoskeleton is a key target in the field poppy SI response, undergoing depolymerization (Snowman et al., 2002) followed by polymerization into highly stable F-actin foci decorated with the actin binding proteins (ABPs) Actin-Depolymerizing Factor (ADF) and Cyclase-Associated Protein (CAP; Poulter et al., 2010, 2011), with both processes being involved in mediating PCD (Thomas et al., 2006). A major player in SI-mediated PCD is a caspase-3-like/DEVDase-like activity (Thomas and Franklin-Tong, 2004; Bosch and Franklin-Tong, 2007). The SI-induced caspase-3-like/DEVDase exhibits maximum substrate cleavage in vitro at pH 5, with peak activity 5 h after SI induction in vivo (Bosch and Franklin-Tong, 2007). The low pH optimum for this caspase-3-like/DEVDase activity is unusual, because most of the cytosolic plant caspase-like activities identified to date have optimal activity close to normal physiological pH (approximate pH, 6.5–7.0; Korthout et al., 2000; Bozhkov et al., 2004; Coffeen and Wolpert, 2004). Because the SI-induced cytosolic-located DEVDase requires a low pH for activity, this suggested that, during SI, the pollen tube cytosol undergoes dramatic acidification. In vivo pH measurements of the cytosol at 1 to 4 h after SI induction confirmed this, when cytosolic pH ($[pH]_{cyt}$) had dropped from pH 6.9 to pH 5.5 (Bosch and Franklin-Tong, 2007). This fits the in vitro pH optimum of the caspase-3-like/DEVDase almost exactly, implicating pollen cytosolic acidification as playing a vital role in creating optimal conditions for the activation of the caspase-3-like/DEVDase-like activity and progression of PCD.

Under normal cellular conditions, $[pH]_{cyt}$ is between approximately 6.9 and 7.5 (Kurkdjian and Guern, 1989; Felle, 2001). Pollen tubes, like other tip-growing cells, have $[pH]_{cyt}$ gradients (Gibbon and Kropf, 1994; Feijó et al., 1999). The $[pH]_{cyt}$ of the pollen tube shank is an approximate pH of 6.9 to 7.11 (Fricker et al., 1997; Messerli and Robinson, 1998). There has been much debate about the $[pH]_{cyt}$ gradient, comprising an apical domain with an approximate pH of 6.8 and a subapical alkaline band with an approximate pH of 7.2 to 7.8 in *Lilium longiflorum* and *Lilium formosanum* pollen tubes (Fricker et al., 1997; Messerli and Robinson, 1998; Feijó et al., 2001; Lovy-Wheeler et al., 2006). Oscillations of $[pH]_{cyt}$ between approximate pH values of 6.9 and 7.3 have been linked to tip growth in *L. formosanum* pollen tubes (Lovy-Wheeler et al., 2006). The vacuole and the apoplast have a highly acidic pH between pH 5 and pH 6 (Katsuhara et al., 1989; Feijó et al., 1999). The majority of studies of pH changes in plant cells reports modest, transient changes in $[pH]_{cyt}$ of approximately 0.4 and 0.7 pH units during development, gravitropic responses, decreases in light intensity, and addition of elicitors, hormones, and other treatments. For example, during root hair development in Arabidopsis (*Arabidopsis thaliana*), root $[pH]_{cyt}$ was elevated from an approximate pH of 7.3 to 7.7 (Bibikova et al., 1998). Root gravitropic responses stimulate small transient $[pH]_{cyt}$ alterations (Scott and Allen, 1999; Fasano et al., 2001; Johannes et al., 2001). More recently, it has been shown that the $[pH]_{cyt}$ drops during PCD controlling root cap development; however, exactly how many units the $[pH]_{cyt}$ decreased was not measured (Fendrych et al., 2014). Other studies investigating $[pH]_{cyt}$ in response to physiologically relevant signals also report small transient alterations. Light-adapted cells respond to a decrease in light intensity with a rapid transient cytosolic acidification by approximately 0.3 pH units (Felle et al., 1986). Addition of nodulation factors resulted in an increase of 0.2 pH units in root hairs (Felle et al., 1998), and abscisic acid increased the $[pH]_{cyt}$ of guard cells by 0.3 pH units (Blatt and Armstrong, 1993). Changes in $[pH]_{cyt}$ are thought to activate stress responses (Felle, 2001). Elicitor treatments resulted in a $[pH]_{cyt}$ drop of between 0.4 and 0.7 pH units in suspension cells (Mathieu et al., 1996; Kuchitsu et al., 1997), a drop of 0.2 pH units in *Nitellopsis obtusa* cells treated with salt (Katsuhara et al., 1989), and a drop of 0.3 to 0.7 pH units in *Eschscholzia californica* (Roos et al., 1998).

Here, we investigate SI-induced acidification of the cytosol, providing measurements of physiologically relevant temporal alterations in $[pH]_{cyt}$, and identify key targets of this, providing mechanistic insights into these events. The SI-induced acidification plays a pivotal role in the activation of a caspase-3-like/DEVDase activity, the formation of punctate F-actin foci, and ABP localization during SI PCD. We investigate the vacuole as a potential contributor to SI-induced $[pH]_{cyt}$ acidification.

RESULTS

Dramatic and Rapid Acidification of Field Poppy Pollen Tube Cytosol Is Stimulated during SI

We previously reported acidification of field poppy pollen tube cytosol after SI induction (Bosch and Franklin-Tong, 2007), but a temporal characterization of this was not carried out. We, therefore, investigated SI-induced $[pH]_{cyt}$ changes at various time points up to 3 h after SI induction using the ratiometric pH indicator 2,7-bis-(2-carboxyethyl)-5-(and-6)-carboxyfluorescein (BCECF) acetoxymethyl ester (AM) and calibrated the $[pH]_{cyt}$ (Supplemental Fig. S1). The time points chosen were 10, 30, 60, and 180 min after SI, because these correspond to when key features of the SI response were observed, particularly the changes in F-actin foci. Typically, small speckles of F-actin are seen at 30 min, and larger F-actin foci are formed between 30 and 60 min post-SI and continue to grow in size (Poulter et al., 2010). Increases in $[Ca^{2+}]_{cyt}$ were virtually instantaneous, and therefore, this is assumed to be the initiating signal; ROS peaks at approximately 5 min and is upstream of actin

alterations. Three hours was chosen as the end point, because this seemed to be the time point when actin foci had fully formed. DEVDase activity was observed much later; a small (nonsignificant) increase was observed at 90 min, and significant increases in activity were observed later at 3 to 5 h (Bosch and Franklin-Tong, 2007; see Wilkins et al., 2014 and Supplemental Fig. S2 for a recent summary of SI-induced events). The $[pH]_{cyt}$ of untreated, growing pollen tubes at time 0 for all treatments was relatively constant at pH 6.8 ± 0.004 ($n = 100$; Fig. 1A). There was no significant difference between the $[pH]_{cyt}$ of untreated pollen tubes and that of compatible pollen tubes at $t = 0$ ($P = 0.871$, $n = 16$). The $[pH]_{cyt}$ of untreated pollen tubes did not change significantly over a period of 3 h ($P = 0.069$, $n = 69$; Fig. 1A); representative images are shown in Supplemental Figure S3, A and B. SI induction resulted in a rapid drop in $[pH]_{cyt}$ (Fig. 1A). Within 10 min, the mean $[pH]_{cyt}$ was 6.4 ± 0.14, which is significantly different from untreated pollen tube $[pH]_{cyt}$ at the same time point ($P = 0.0001$, $n = 11$); 30 min after SI induction, the $[pH]_{cyt}$ of incompatible pollen tubes had decreased to pH 6.0 ± 0.10. Acidification continued for up to 60 min, when it reached $[pH]_{cyt}$ of 5.5 ± 0.12, which was significantly different than that of untreated pollen tubes at 60 min ($P = 8.32 \times 10^{-6}$, $n = 16$; Supplemental Fig. S3, B and E). The $[pH]_{cyt}$ of incompatible pollen tubes at 60 min post-SI induction was similar to that at 180 min ($P = 0.105$, $n = 26$; Fig. 1A), which suggested that the cytosol had reached a $[pH]_{cyt}$ equilibrium. The acidification was SI specific, because the $[pH]_{cyt}$ of compatible pollen tubes treated with PrsS remained at an approximate pH of 7.0 ± 0.04 throughout and did not significantly differ from the $[pH]_{cyt}$ of untreated samples ($P = 0.168$, $n = 8$; Fig. 1). These data show that SI induction triggers dramatic and rapid acidification of the pollen tube cytosol in an *S*-specific manner.

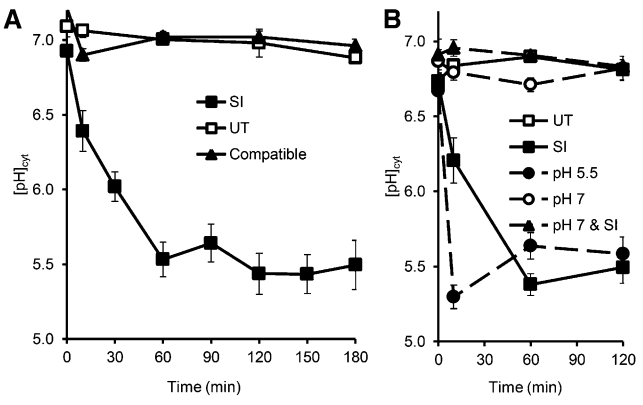

Figure 1. SI-induced pollen tubes undergo rapid cytosolic acidification, and artificial alteration of pollen tube $[pH]_{cyt}$ can mimic and prevent SI-induced acidification. A, Pollen tubes labeled with the pH indicator BCECF AM were treated with either PrsS to provide an incompatible response (SI; $n = 152$) or a compatible response (compatible; $n = 32$) or untreated (UT; $n = 69$). B, Pollen tubes labeled with BCECF AM were incubated with 50 mM propionic acid (pH 7, $n = 57$; or pH 5.5, $n = 62$), pretreated with pH 7 for 10 min before SI induction (pH 7 & SI; $n = 29$), or untreated ($n = 70$).

Manipulation of Pollen Tube $[pH]_{cyt}$ Using Propionic Acid Can Mimic or Prevent SI-Induced Acidification

To investigate the role of SI-induced cytosolic acidification, 50 mM propionic acid was used to manipulate the pollen tube $[pH]_{cyt}$. We did not measure the growth rates, because after propionic acid treatment, growth was stopped immediately, although cytoplasmic streaming continued, indicating that pollen tubes were still alive and viable. This has been documented in other publications (Parton et al., 1997), where acidification or alkalinization of the cytoplasmic pH of *Agapanthus* spp. pollen tubes and *Dryopteris* spp. rhizoids using propionic acid completely inhibited growth.

Addition of propionic acid (pH 5.5) resulted in rapid $[pH]_{cyt}$ acidification and mimicked SI-induced acidification (Fig. 1B); within 10 min, the $[pH]_{cyt}$ was 5.3 ± 0.1 ($n = 17$), significantly different from untreated samples ($P = 1.49 \times 10^{-7}$, $n = 22$). After 120 min, the $[pH]_{cyt}$ was not significantly different to that of SI-induced pollen tubes ($P = 0.691$, $n = 8$). The $[pH]_{cyt}$ of pollen tubes incubated with propionic acid (pH 7) did not significantly change over 120 min compared with that of untreated pollen ($P = 0.875$, $n = 5$).

To examine if the SI-induced acidification could be prevented, pollen tubes were treated with 50 mM propionic acid (pH 7) for 10 min before SI induction, and $[pH]_{cyt}$ was monitored. Ten minutes after SI induction, pretreated samples had a $[pH]_{cyt}$ 6.9 ± 0.0 ($n = 4$); after 120 min, the $[pH]_{cyt}$ was similar to the initial $[pH]_{cyt}$ ($P = 1.00$, $n = 9$) and untreated samples ($P = 0.705$, $n = 8$; Fig. 1B). The $[pH]_{cyt}$ of SI-induced pollen was significantly different from that of pH 7-pretreated pollen tubes at 120 min post-SI ($P = 5.32 \times 10^{-4}$, $n = 8$). This shows that propionic acid (pH 7) can prevent SI-induced acidification.

Manipulation of Pollen Tube $[pH]_{cyt}$ Can Trigger or Prevent DEVDase Activity

Caspase-3-like/DEVDase activity is a key feature of SI-induced PCD. Previous characterization revealed that its peak activity, which is observed to increase between 3 and 5 h after SI induction, has a very narrow pH range (approximate pH, 4.5–5.5; Bosch and Franklin-Tong, 2007). Having established that SI-induced $[pH]_{cyt}$ dropped very rapidly, we wished to explore whether this affected pollen tube cytosolic DEVDase activity. We used propionic acid to alter $[pH]_{cyt}$ and measured caspase-3-like/DEVDase activity at 5 h post-SI induction using the live-cell caspase-3 probe carboxyfluorescein-DEVD-fluoromethylketone Fluorescent-Labeled Inhibitor of Caspases (FAM-DEVD-FMK FLICA). SI-induced pollen tubes at 5 h post-SI induction displayed fluorescence, indicating caspase-3/DEVDase activity (Fig. 2, A and B), unlike untreated pollen tubes (Fig. 2, C and D). We investigated whether the addition of propionic acid (pH 5.5; mimicking SI-induced acidification) could stimulate caspase-3/DEVDase activity and if pretreatment with propionic acid (pH 7) before SI induction prevented it.

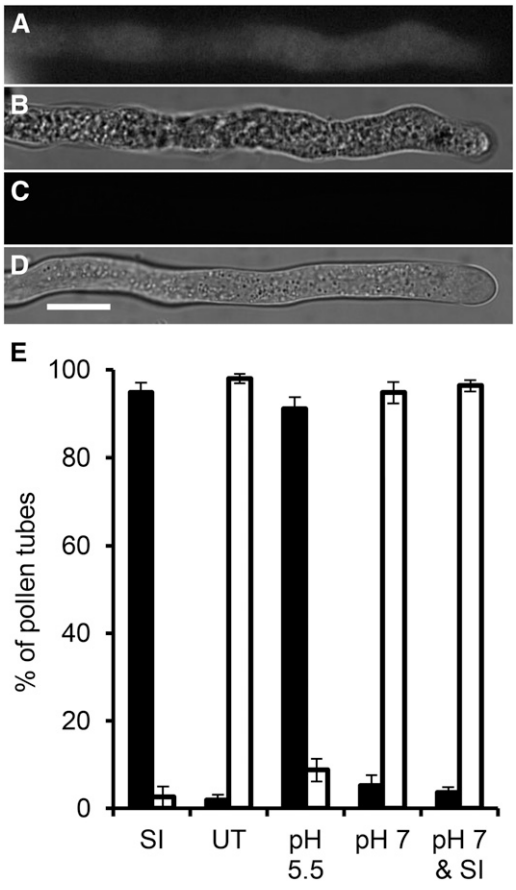

Figure 2. Pollen tube $[pH]_{cyt}$ can activate or prevent DEVDase/caspase-3-like activity. A, Representative pollen tube after SI induction labeled with FAM-DEVD-FMK FLICA exhibits fluorescence, indicating DEVDase/caspase-3-like activity. B, Bright-field image of A. C, Representative untreated pollen tube labeled with FAM-DEVD-FMK FLICA exhibits no fluorescence. D, Bright-field image of C. All images are 5 h after treatment. Bar = 10 μm. E, Quantitation of 150 pollen tubes scored positive (black bars) or negative (white bars) for fluorescence, indicating DEVDase/caspase-3-like activity, after the following treatments: SI induction (SI); growth medium (UT); 50 mM propionic acid, pH 5.5 (pH 5.5); 50 mM propionic acid, pH 7 (pH 7); or 10-min pretreatment with 50 mM propionic acid (pH 7) followed by SI induction (pH 7 & SI) incubated for 5 h before the addition of FAM-DEVD-FMK FLICA.

Quantitation revealed that almost all (97%) SI-induced pollen tubes exhibited caspase-3-like/DEVDase activity, unlike untreated pollen tubes (3%; Fig. 2E). Addition of propionic acid (pH 5.5) resulted in many pollen tubes with caspase-3-like/DEVDase activity (not significantly different from SI-induced samples; P = 0.331). Treatment with propionic acid (pH 7) alone was not significantly different from untreated samples (P = 0.26). Importantly, pretreatment with propionic acid (pH 7) before SI induction gave low numbers (5%) of pollen tubes with caspase-3/DEVDase activity, significantly different from those treated with propionic acid (pH 5.5; $P = 1.6 \times 10^{-9}$; Fig. 2E). These data show that acidification of the pollen tube cytosol is required for the activation of caspase-3-like/DEVDase activities and identifies a strong link between pollen tube $[pH]_{cyt}$ and initiation of PCD.

Acidification of Field Poppy Pollen Tube Cytosol Triggers F-Actin Foci

We previously showed that the actin cytoskeleton is a key target in the field poppy SI response, undergoing depolymerization (Snowman et al., 2002) followed by polymerization into highly stable F-actin foci (Poulter et al., 2010, 2011), with both processes being involved in mediating PCD (Thomas et al., 2006). We wondered if the SI-induced acidification might play a role in mediating some of these changes. To investigate this, we used propionic acid to manipulate the $[pH]_{cyt}$ of pollen tubes. Normally growing pollen tubes had typical longitudinal bundled actin filament organization (Fig. 3A). Incompatible pollen tubes after 3 h of SI induction had many F-actin foci (Fig. 3B). Pollen tubes treated with propionic acid (pH 5.5) for 3 h also had numerous F-actin foci (Fig. 3C). Pollen tubes treated with propionic acid (pH 7) had an actin configuration similar to untreated pollen tubes (Fig. 3D) as did pollen tubes pretreated with propionic acid (pH 7) before SI induction. Quantification revealed that propionic acid (pH 5.5) resulted in significantly more pollen tubes with F-actin foci than untreated samples ($P = 1.08 \times 10^{-11}$) or those treated with propionic acid (pH 7; $P = 5.98 \times 10^{-4}$; Fig. 3E). Preventing SI-induced acidification with propionic acid (pH 7) resulted in significantly fewer pollen tubes with F-actin foci than observed in SI-induced samples ($P = 8.30 \times 10^{-8}$; Fig. 3E), but it was not significantly different from those treated with propionic acid (pH 7) alone (P = 0.114). Thus, lowering the pollen tube $[pH]_{cyt}$ to pH 5.5 can trigger the formation of F-actin foci. Moreover, preventing acidification in SI-induced pollen tubes prevented their formation. This shows the functional importance of acidification in the SI response in field poppy pollen tubes and gives us an insight into mechanisms involved in their formation.

Acidification of the Cytosol Triggers Colocalization of CAP and ADF with F-Actin Foci

To understand mechanisms involved in F-actin foci formation, we used propionic acid to investigate the effect of pH on the localization of two ABPs: ADF/cofilin and CAP (Poulter et al., 2010). Pollen was treated with propionic acid, and F-actin was visualized using rhodamine-phalloidin together with immunolocalization with antibodies directed against either CAP or ADF. Normally growing pollen tubes had typical longitudinal bundled actin filament organization and cytosolic-localized CAP and ADF (Supplemental Fig. S4, A–F). Incompatible pollen tubes after 3 h of SI induction had large F-actin foci that colocalized with CAP and ADF (Supplemental Fig. S4, G–L). Pollen tubes treated with propionic acid (pH 7) had an actin configuration similar to untreated pollen tubes (Supplemental

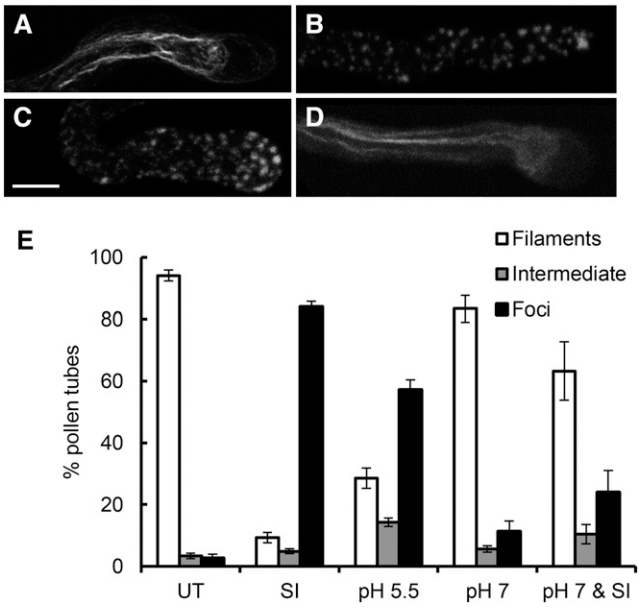

Figure 3. Acidification of the pollen tube cytosol triggers the formation of punctate F-actin foci. Representative images of pollen tubes showing F-actin labeled with rhodamine-phalloidin for F-actin visualization after 3 h of treatment with untreated pollen tube (A), SI-induced pollen tube (B), pH 5.5 propionic acid-treated pollen tube (C), or pH 7.0 propionic acid-treated pollen tube (D). Bar = 10 μm. E, Quantification of pollen tubes treated as above. Pollen tubes were scored for F-actin in categories showing untreated (UT) phenotype (filaments; white bars), an SI phenotype (foci; black bars), or an intermediate phenotype (intermediate; gray bars). n = 650 per treatment over 10 independent repeats.

Fig. S4, M–R) as did pollen tubes pretreated with propionic acid (pH 7) before SI induction. Pollen tubes treated with propionic acid (pH 5.5) for 3 h also had large F-actin foci, typical of SI induction that colocalized with CAP and ADF (Supplemental Fig. S4, S–X).

Quantification of F-actin and CAP colocalization (Fig. 4A) showed that, in untreated pollen tubes, colocalization of F-actin and CAP was minimal (3.7% of untreated pollen tubes showed some colocalization) and significantly different from SI-induced pollen tubes (80%; $P = 9.88 \times 10^{-5}$). Pollen treated with propionic acid (pH 5.5) resulted in high levels of F-actin foci and CAP colocalization, which was significantly different from untreated pollen ($P = 1.23 \times 10^{-4}$). Pretreatment of pollen tubes with propionic acid (pH 7) before SI induction resulted in significantly lower occurrence of F-actin foci and CAP colocalization compared with SI alone (45% of SI-induced pollen tubes; $P = 8.25 \times 10^{-4}$) and compared with pollen treated with propionic acid (pH 5.5; $P = 0.004$). Propionic acid (pH 7) gave low levels of F-actin foci, similar to untreated pollen tubes. Similar results were obtained for colocalization of F-actin and ADF for these treatments (Fig. 4B). In untreated pollen tubes, colocalization of F-actin foci and ADF was minimal (4%) and significantly different from that in SI-induced pollen tubes (80%; $P = 6.44 \times 10^{-6}$). Addition of propionic acid (pH 5.5) gave high levels of F-actin foci, which was significantly different to untreated pollen ($P = 4.06 \times 10^{-6}$). Pretreatment with propionic acid (pH 7) before SI induction resulted in a lower occurrence of F-actin with colocalized ADF foci compared with SI-induced pollen tubes (48% of SI samples; $P = 1.86 \times 10^{-4}$) and compared with pH 5.5-treated pollen tubes ($P = 0.002$). Pollen treated with propionic acid (pH 7) alone had similar levels of actin foci with colocalized ADF to untreated samples ($P = 0.100$). This shows that lowering the $[pH]_{cyt}$ to 5.5 stimulates both the formation of F-actin foci and the colocalization of both CAP and ADF to these structures, providing in vivo evidence that the cellular localization of both CAP and ADF is affected by $[pH]_{cyt}$ acidification.

Altered pH Dramatically Affects sPPase Activity

We previously identified two pollen-expressed sPPases, Prp26.1a and Prp26.1b, that are modified by phosphorylation early in the SI response (Rudd et al., 1996; de Graaf et al., 2006). We wished to establish the effect of the SI-induced pH alterations on these important cytosolic enzymes by testing their activities within the range of SI-induced pH alterations in incompatible pollen

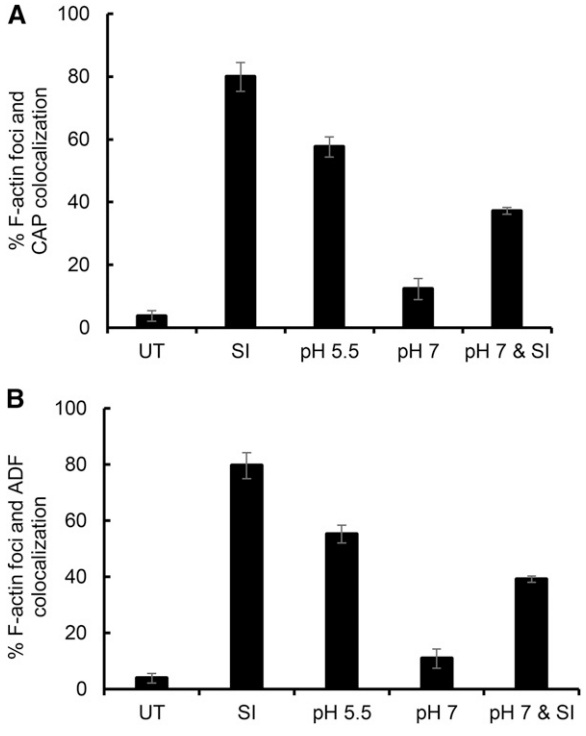

Figure 4. Acidification of the pollen tube cytosol triggers the formation of punctate F-actin foci and colocalization of CAP and ADF. A, Quantification of F-actin and CAP colocalization. Pollen tubes were scored for actin foci and CAP colocalization in three independent experiments (n = 700 per treatment over three independent repeats). B, Quantification of F-actin and ADF colocalization. Pollen tubes were scored for actin foci and ADF colocalization in three independent experiments (n = 700 per treatment over three independent repeats). UT, Untreated.

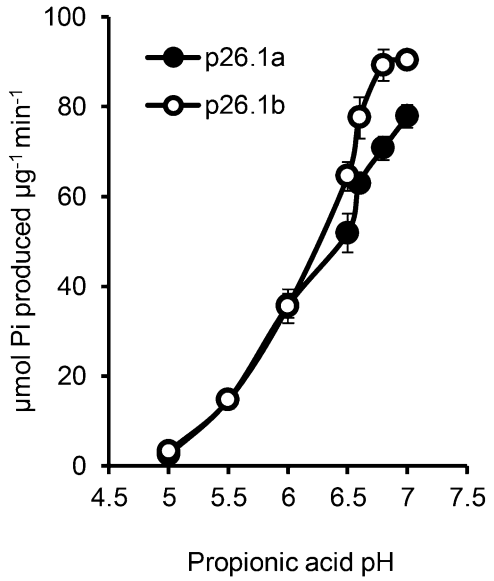

Figure 5. pH dramatically affects sPPase activity. Recombinant p26.1a and p26.1b sPPase samples were assayed in 50 mM propionic acid (pH 5–7.5) in the presence of 2 mM $Na_4P_2O_7$ as a substrate, and the amount of inorganic phosphorous (Pi) released was measured ($n = 4$).

tubes. At the normal physiological $[pH]_{cyt}$ of pollen tubes at pH 7, there was high sPPase activity (77.82 ± 2.8 and 90.4 ± 1.6 for Prp26.1a and Prp26.1b, respectively; Fig. 5). At an approximate pH of 6.5, which corresponds to the $[pH]_{cyt}$ of incompatible pollen tubes approximately 10 min post-SI, the sPPase activities of Prp26.1a and Prp26.1b were reduced to 40.4% and 58.3%, respectively, of their original activities ($P = 0.029$ and $P \leq 0.001$, respectively; Fig. 5). At pH 6.0, the $[pH]_{cyt}$ at 30 min post-SI, the sPPase activities were reduced further to 36.0 ± 2.7 and 36.0 ± 3.8, respectively ($P \leq 0.001$ and $P < 0.001$, respectively). At pH 5.5 (the $[pH]_{cyt}$ at 60 min post-SI), sPPase activities were negligible at only 11.4% and 13.2%, respectively, of their original activity at pH 7 (both $P \leq 0.001$; Fig. 5). This shows that the SI-induced acidification has a dramatic effect on sPPase activities and most likely, many other important cytosolic enzymes. This suggests that, within a few minutes of the SI response, many key enzymes required for pollen tube function are likely to be inactivated.

SI Triggers Vacuolar Reorganization and Disintegration

Vacuolar rupture is implicated as a key, irreversible step in several plant PCD systems (van Doorn et al., 2011). Because the vacuole is a major acidic organelle in plant cells, we wished to investigate whether it might be involved in the SI PCD response. We used the vacuolar marker carboxy-5-(and-6)-carboxy-2′,7′-dichlorofluorescein diacetate (carboxy-DCFDA) to label the pollen tube vacuole. The vacuole of untreated growing pollen tubes has a reticulate structure throughout the pollen tube shank, absent in the apical region (Fig. 6A; Supplemental Movie S1). SI-induced pollen tubes displayed vacuolar reorganization within 15 min with small aggregations (Fig. 6A). As SI progressed, the typical reticulate structure was lost (Fig. 6A); later, there was additional aggregation and a decrease in vacuolar labeling, suggesting breakdown. After 118 min, very little intact structure remained (Fig. 6A). Scoring vacuolar morphology revealed that 80% of pollen tubes had undergone some form of reorganization within 15 min ($n = 63$), and within 30 to 50 min, 77% ($n = 35$) had undergone extensive breakdown (Supplemental Fig. S5). To be confident that the carboxy-DCFDA probe was reporting the vacuole, δ-Tonoplast Intrinsic Protein (TIP)-GFP, which labels the vacuolar membrane (Hicks et al., 2004), was used. The δ-TIP-GFP reported a similar reticulate pattern to that observed with carboxy-DCFDA, and by 89 min after SI induction, there was very little intact vacuolar signal remaining (Fig. 6B; Supplemental Movie S2). This provides confidence that carboxy-DCFDA reports the vacuole and shows that SI triggers vacuolar reorganization/breakdown.

Artificial Manipulation of $[pH]_{cyt}$ of Pollen Tube Triggers Vacuolar Alterations

We wished to examine the relationship between the vacuole and cytosolic acidification further. We used propionic acid to alter $[pH]_{cyt}$ and monitored vacuolar organization using carboxy-DCFDA. No reorganization was observed in untreated pollen tubes within 80 min (Fig. 6C; Supplemental Fig. S6A). SI induction resulted in reorganization and apparent breakdown of the vacuole after 85 min (Fig. 6C). Pollen tubes treated with propionic acid (pH 5.5) showed dramatic disintegration of the vacuole ($n = 6$; Fig. 6C; Supplemental Fig. S6B). This shows that cytosolic acidification has a major effect on the pollen tube vacuole. Contrary to our expectation that vacuolar breakdown would result in acidification of the $[pH]_{cyt}$, acidification of the cytosol actually triggered vacuolar breakdown. This suggests that there may be an earlier acidification event before vacuolar breakdown. We also investigated whether maintaining the $[pH]_{cyt}$ might prevent vacuolar breakdown. Pollen tubes treated with propionic acid (pH 7) for 10 min before SI induction exhibited only slight reorganization of the carboxy-DCFDA vacuolar signal (Fig. 6C; Supplemental Fig. S6C). This provides evidence that maintaining the pollen tube $[pH]_{cyt}$ can prevent vacuolar breakdown but not reorganization and suggests that there is a signal upstream of vacuolar alterations, which triggers breakdown. Together, these data suggest that the initial SI-induced acidification of the cytosol is upstream of SI-induced vacuolar breakdown.

The Ca^{2+} Ionophore A23187 Triggers Cytosolic Acidification and Vacuolar Reorganization

Because the $[pH]_{cyt}$ alterations were unexpectedly rapid, we wondered whether increases in $[Ca^{2+}]_{cyt}$ might trigger acidification, because SI triggers almost instantaneous, transient increases in pollen tube $[Ca^{2+}]_{cyt}$ and Ca^{2+} influx (Franklin-Tong et al., 1997; Wu et al., 2011). Pollen

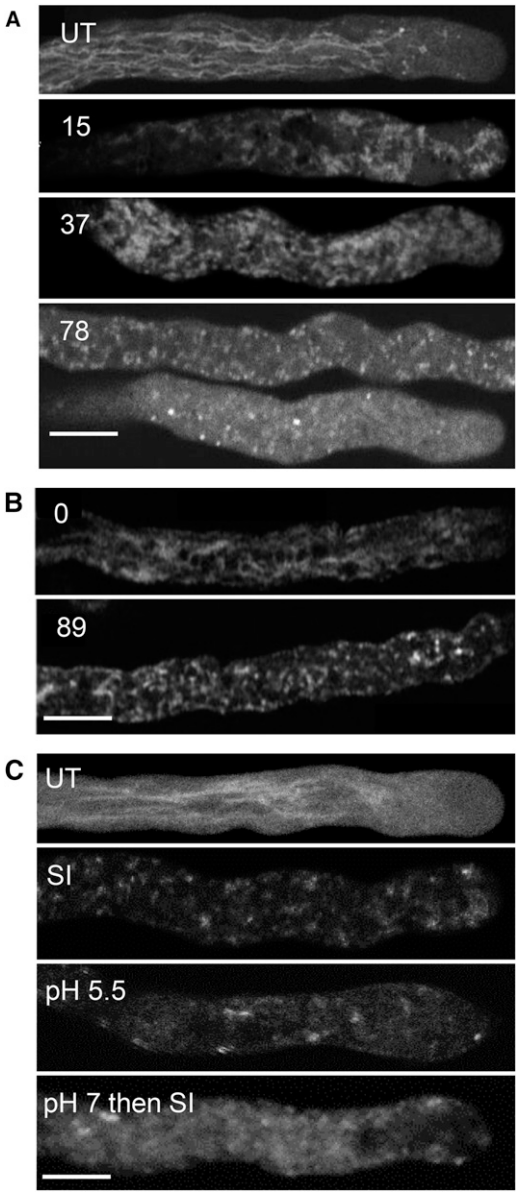

Figure 6. SI triggers pollen tube vacuolar reorganization and disintegration, and artificial acidification of the cytosol triggers alterations in vacuolar organization. A, Pollen tubes labeled with 1 μM carboxy-DCFDA were SI induced and imaged using confocal microscopy. Numbers indicate the length of treatment time in minutes: t = 15 min indicates that the vacuolar network has reorganized, t = 37 min indicates additional vacuolar reorganization, and t = 78 min indicates that the vacuolar structure appears disintegrated. UT, Typical untreated pollen tube with a tubular vacuole organization. B, Stills from a time series of a pollen tube expressing δ-TIP-GFP: t = 0 indicates typical membrane-localized reticulate structure, and t = 89 min indicates that, after SI induction, there is apparent reorganization and only a dispersed, punctate signal remains. C, Field poppy pollen tubes were labeled with carboxy-DCFDA and imaged using confocal microscopy after the following treatments: UT, Untreated; SI, SI-induced pollen tube for t = 76 min; pH 5.5, 50 mM propionic acid (pH 5.5)-treated pollen tube for t = 85 min; pH 7 then SI, pollen tube pretreated with 50 mM propionic acid (pH 7.0) for t = 10 min followed by SI induction for t = 68 min. Bars = 10 μm.

tubes were treated with the Ca^{2+} ionophore A23187, and the $[pH]_{cyt}$ was monitored. Addition of A23187 resulted in rapid acidification of the $[pH]_{cyt}$ (Fig. 7A). Within 30 min, there was a significant difference in $[pH]_{cyt}$ of A23187-treated pollen tubes compared with untreated pollen tubes (P = 0.003, n = 12). After 60 min, $[pH]_{cyt}$ had dropped to pH 5.69 $\pm$ 0.17 (n = 8), and after 120 min, the $[pH]_{cyt}$ had dropped further and was significantly different to that of untreated pollen tubes at the same time point ($P = 6.33 \times 10^{-9}$; Fig. 7A). This shows that the Ca^{2+} ionophore A23187 can trigger rapid major acidification, suggesting that the influx of Ca^{2+} (and possibly other ions) is upstream of acidification and may be implicated in triggering SI-induced acidification of the pollen tube cytosol.

To establish whether increases in $[Ca^{2+}]_{cyt}$ might trigger vacuolar changes, we investigated the effect of A23187 on the pollen tube vacuole using carboxy-DCFDA (Fig. 7B). Seven minutes after addition of A23187, the reticulate structure observed in untreated pollen tubes had undergone some reorganization. Within 25 min, the vacuolar signal had formed large aggregates, and an increased cytosolic-located signal suggested leakage of the dye and vacuolar rupture. By 46 and 77 min after the addition of A23187, there was very little vacuolar signal remaining (Fig. 7B). A23187-stimulated breakdown of the vacuole appeared similar to the SI-induced alterations that were observed. This places Ca^{2+} influx and increases in $[Ca^{2+}]_{cyt}$ (as well as other ions; possibly H^+) as very early signals that occur upstream of vacuolar breakdown.

DISCUSSION

SI Triggers a Dramatic Drop in $[pH]_{cyt}$

We previously reported dramatic cytosolic acidification triggered by SI (Bosch and Franklin-Tong, 2007). This was the first report, to our knowledge, of PCD-associated cytosolic acidification in plants. Here, we have investigated SI-induced acidification of the cytosol in detail. We measured the temporal alterations in $[pH]_{cyt}$ and provide evidence showing its biological relevance and identifying targets and intracellular consequences of the SI-induced acidification. We show that acidification of the $[pH]_{cyt}$ plays a pivotal role in SI-induced PCD by creating optimal conditions for activation of the DEVDase/caspase-3-like activity, which has optimal activity between pH 4.5 and pH 5.5 and negligible activity above pH 6.0 (Bosch and Franklin-Tong, 2007). Acidification also plays a crucial role in the formation of punctate F-actin foci, most likely by altering the localization and activity of at least two ABPs, ADF and CAP. The scale of the drop in $[pH]_{cyt}$ triggered by SI is notable. Although many measurements of alterations in $[pH]_{cyt}$ exist in various plant cell systems, most of the alterations are rather small and on the scale of <1.0 pH unit. Below, we consider some of the cellular processes that are affected by this major change in cellular homeostasis.

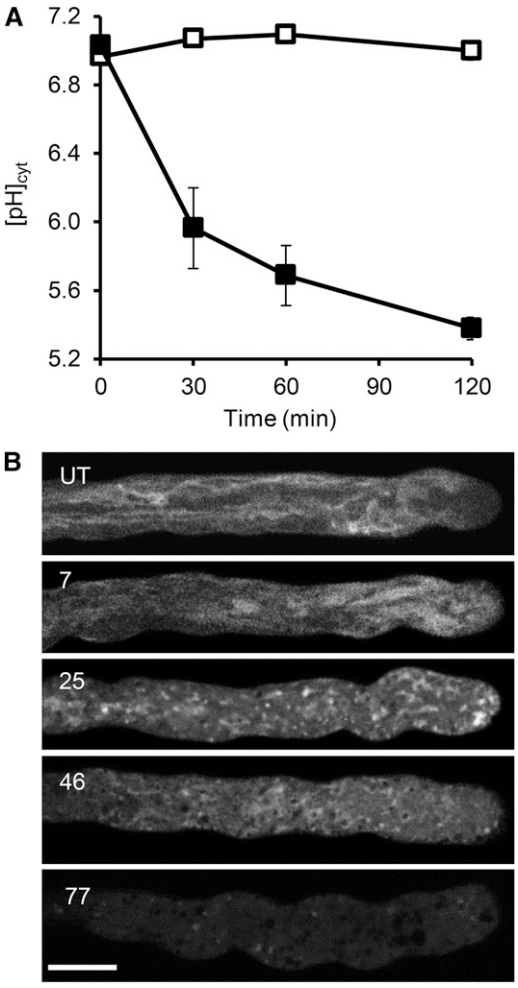

Figure 7. Ca^{2+} ionophore A23187 triggers cytosolic acidification and vacuolar reorganization of field poppy pollen tubes. A, Fifty micromolar A23187 (black symbols; $n = 27$) or growth medium (white symbols; $n = 25$) was added to field poppy pollen tubes growing in vitro, and pH was measured and calibrated with the ratiometric pH indicator BCECF AM. B, Pollen tubes were treated with 10 μM A23187 and labeled with carboxy-DCFDA to visualize the vacuole. Numbers indicate the length of treatment time in minutes: 7 min after the addition of A23187, the vacuole still shows some reticulate appearance; 25 min after the addition of A23187, there is major reorganization with appearance of collapse/aggregation; 46 min after the addition of A23187, little structure is apparent; and 77 min after the addition of A23187, reduced signal suggests extensive breakdown of the vacuole. UT, Typical untreated pollen tube exhibits a reticulate structure. Bar = 10 μM.

A Drop in $[pH]_{cyt}$ Is Necessary and Sufficient for PCD

We have shown using propionic acid that a drop in $[pH]_{cyt}$ to pH 5.5 is sufficient to trigger a caspase-3-like/DEVDase activity in field poppy pollen tubes and that maintaining $[pH]_{cyt}$ at pH 7 is sufficient to prevent entry into PCD. This shows that the drop in $[pH]_{cyt}$ is a pivotal event in the SI-induced PCD. Contrary to expectation, there are surprisingly few measurements of $[pH]_{cyt}$ during PCD in any plant system. To our knowledge, with the exception of our previous study (Bosch and Franklin-Tong, 2007) and the results described here, no measurements of $[pH]_{cyt}$ exist to show the extent of the acidification of $[pH]_{cyt}$ during PCD in plants. One of the few studies to monitor pH alterations during PCD in plants is a recent study by Young et al. (2010), which measured loss of fluorescence of the pH-sensitive Yellow Fluorescent Protein probe as an indication of change in $[pH]_{cyt}$. A similar methodology was used to show that the $[pH]_{cyt}$ dropped during root cap developmental PCD (Fendrych et al., 2014). However, neither study was calibrated to give an indication of the actual $[pH]_{cyt}$ range. Our study confirms that acidification can trigger PCD in another plant system, suggesting that it may be a general phenomenon worth investigating in other PCD systems to determine how widespread this control might be.

The Involvement of the Vacuole in Cytosolic Acidification and SI-Mediated PCD

The vacuole is a very acidic organelle, with a pH of approximately 5 (Shen et al., 2013). Vacuolar breakdown is a common feature of PCD in plants (Fukuda, 2000; Jones, 2001; Hara-Nishimura and Hatsugai, 2011) and one of two major classes of plant PCD (van Doorn et al., 2011). It is thought that collapse of the vacuole is a key, irreversible step in several plant PCD systems, and vacuolar rupture is often used to mark the death of a cell. However, how this is achieved and what processes are involved remain unknown. Vacuoles accumulate hydrolases, which are released into the cytoplasm upon vacuolar rupture. This is thought to be important for eliminating the cell corpse and recycling cellular material (Jones, 2001). During tracheary element differentiation, the vacuole ruptures virtually instantaneously and marks a point of no return, releasing enzymes into the cytosol that contribute to the degradation of the cell (Obara et al., 2001; Rotari et al., 2005). During the hypersensitive response in cryptogein-induced cell death in tobacco (*Nicotiana tabacum*) Bright Yellow-2 cells, disruption of vacuolar organization with formation of bulb-like structures and alterations in F-actin organization were observed (Higaki et al., 2007). This latter report seems similar to the SI-induced events, which involve the actin cytoskeleton (Snowman et al., 2002; Wilkins et al., 2014). We, therefore, expected to observe alterations in the vacuole during the SI response and initially thought that vacuolar breakdown might be responsible for the dramatic acidification of the cytosol. Surprisingly, before the study by Fendrych et al. (2014) and this study, this does not seem to have been investigated. Although vacuolar breakdown occurs during SI, to our surprise, significant cytosolic acidification occurred very early and before observable vacuolar breakdown. Moreover, alterations in $[pH]_{cyt}$ can mediate vacuolar breakdown. This suggests that the initial acidification of the cytosol may not be caused by loss of vacuolar integrity. Thus, although the vacuole is expected to contribute to SI-induced acidification of the cytosol, a drop in $[pH]_{cyt}$ initiates events. Our findings confirm those in Fendrych et al., 2014, which recently showed that the $[pH]_{cyt}$ of the root cap

cells dropped before vacuolar collapse, suggesting that PCD in these two systems is pH activated. This merits examination in additional PCD systems to establish if acidification is a general phenomenon and how it is achieved.

Signaling to SI-Induced PCD

Ca^{2+} operates as a second messenger in many signaling cascades in both plant and animal systems, including PCD (Rudd and Franklin-Tong, 1999). $[Ca^{2+}]_{cyt}$ is known to play a pivotal signaling role in incompatible field poppy pollen; increased $[Ca^{2+}]_{cyt}$ is the earliest event triggered by SI (Franklin-Tong et al., 1993; Wu et al., 2011) that involves Ca^{2+} influx (Wu et al., 2011). Vacuolar collapse in several PCD systems requires increases in $[Ca^{2+}]_{cyt}$; artificially inducing Ca^{2+} influx can trigger the collapse of the vacuole in cells competent to undergo PCD (Jones, 2001). Here, we have shown that A23187 can trigger both cytosolic acidification and vacuolar breakdown. $[Ca^{2+}]_{cyt}$ is known to play a pivotal signaling role in incompatible field poppy pollen. The SI signaling events can be classified into two categories. Signal initiation events include increases in $[Ca^{2+}]_{cyt}$ (Franklin-Tong and Franklin, 1993; Franklin-Tong et al., 1997), Ca^{2+} and K^+ influx (Wu et al., 2011), inhibition of sPPase activity (Rudd et al., 1996; de Graaf et al., 2006), depolymerization and stabilization of F-actin (Snowman et al., 2002; Thomas et al., 2006; Poulter et al., 2008, 2011), and rapid inhibition of incompatible pollen tube growth. These feed into later suicide signaling events involved in commitment to PCD through the activation of caspase-3-like/DEVDase activities. Events include activation of the p56 MAPK (Rudd et al., 2003; Li et al., 2007), increases in ROS (Wilkins et al., 2011), and formation of F-actin foci (Poulter et al., 2010, 2011; Wilkins et al., 2011; for review, see Wilkins et al., 2014). Collectively, these signals trigger suicide signaling events leading to a gateway, around 10 min, that incompatible pollen must pass to become irreversibly inhibited and killed. We have previously shown that PrsS can be applied and washed out and that the response of the initial Ca^{2+} influx is fully reversible (Rudd and Franklin-Tong, 2003; Wu et al., 2011). Downstream of this, we previously noted that we can wash out the PrsS within 9 min and gain back pollen tube growth (Rudd and Franklin-Tong 2003). Actin alterations are usually very dynamic, allowing rapid responses to stimuli. There is clearly a key role for the actin cytoskeleton as a sensor of cellular stress, and we have shown previously that we could significantly alleviate PCD by preventing some of the very early, rapid actin depolymerization by adding jasplakinolide (Thomas et al., 2006). This shows that early SI-induced actin alterations play a functional role in the initiation of PCD and are reversible. It is worth noting that it has been proposed that, in animal cells, it is the alteration of actin dynamics (i.e. the rate of actin polymerization and depolymerization) that modulates the transduction of the apoptotic signal (Morley et al., 2003). The formation and the unusual stability of the F-actin foci may contribute to ensuring that entry into PCD becomes irreversible. We propose that the formation of the F-actin foci is both a marker and consequence of signals to PCD and predict that they are not reversible, because they start to form later, around 10 to 30 min, and are unusually stable. Cytosolic acidification could contribute to the gateway, when the drop in $[pH]_{cyt}$ passes a threshold beyond which homeostasis cannot be maintained. The temporal events of cytosolic acidification precede the DEVDase activation by at least 1 h. We suggest that this creates an environment whereby the DEVDase can be activated. If the cleavage of this enzyme is as we would expect, this would gradually increase as a feed-forward loop over time, gradually increasing in activity. Thus, we propose that cytosolic acidification alters cytosolic conditions so that the DEVDase (which has no activity at physiological pH 7) can be activated. There may be other events that trigger initial cleavage and activation of the DEVDase. Thus, the drop in $[pH]_{cyt}$ is pivotal in coordinating SI-induced PCD.

Identification of Targets for pH Alterations

Many cellular processes are regulated by pH. Alterations in $[pH]_{cyt}$ can result in the modification of enzymes and alterations to the structure and activity of ABPs (Gungabissoon et al., 1998; Lovy-Wheeler et al., 2006). Here, we have shown that a drop in $[pH]_{cyt}$ can inhibit or activate enzyme activity and that the configuration of the F-actin cytoskeleton can be altered by a drop in $[pH]_{cyt}$. Our data provide important information about some of the early events that are affected and instrumental in pushing a cell into a PCD pathway and irreversible death. Below, we discuss some of the targets for the dramatic SI-induced reduction in $[pH]_{cyt}$.

We found that the activity of a key enzyme required for cellular biosynthesis and growth, an sPPase p26.1a/p26.1b, was drastically inhibited at pH 6.0 (achieved within 30 min of SI induction) and virtually completely inhibited at pH 5.5. We previously identified this protein as a target for SI signals, being rapidly modified by phosphorylation and inhibited by increases in Ca^{2+}. Here, we have identified a third SI mechanism whereby this sPPase can be inhibited, namely pH. Although we have only measured the effect of a drop in $[pH]_{cyt}$ on the activity of just one enzyme, it is likely that not just sPPase activity is affected by the SI-induced acidification. Many enzymes operate within a narrow pH range, close to the physiological norm of an approximate pH of 7; not surprisingly, they will be inhibited if the $[pH]_{cyt}$ is shifted so dramatically. This very obvious event has not previously been widely examined or discussed in the context of PCD.

Another target of SI-mediated PCD is the actin cytoskeleton, which undergoes rapid depolymerization (Snowman et al., 2002) and then, accumulation and stabilization into punctate actin foci (Poulter et al., 2010); both of these processes seem to be intimately involved in PCD (Thomas et al., 2006). The SI-induced F-actin foci are unusually stable and a hallmark feature of SI PCD (Poulter et al., 2010). Reconfiguration of the actin

cytoskeleton is modulated by ABPs, and we previously showed that, within 10 min of SI induction, ABPs ADF/cofilin and CAP colocalized with these highly stable F-actin foci (Poulter et al., 2010). It is rather surprising to observe ADF and CAP associated with the stable foci, because they are well-characterized key mediators of actin filament depolymerization (Staiger et al., 2010). However, numerous in vitro studies have shown that ADFs exhibit pH-sensitive activity. In general, ADF binding alters actin dynamics by severing actin filaments, providing more ends for polymerization, and increasing the rate of dissociation of actin monomer from the pointed ends (Carlier et al., 1997; Bamburg et al., 1999; Maciver and Hussey, 2002). The activity of most ADFs, including those in plants, is pH sensitive, with preferential binding of F-actin at pH 6.0 to pH 6.5 and G-actin above pH 7.4 (Carlier et al., 1997; Gungabissoon et al., 1998; Allwood et al., 2002). In vitro studies showed that maize (*Zea mays*) ZmADF3 is pH sensitive, cosedimenting with F-actin at pH 6 (Gungabissoon et al., 1998). The activity of LlADF1 from *L. longiflorum* pollen is pH sensitive; at pH 6, LlADF1 was predominantly in the pellet bound to F-actin, indicating low actin-depolymerizing activity, and tobacco NtADF1 depolymerized F-actin in vitro more efficiently at pH 8 than at pH 6 (Chen et al., 2002). ADF-depolymerizing activity increased at more alkaline pHs (Allwood et al., 2002; Chen et al., 2002). A hypothesis proposed is that, in a physiologically relevant, cellular context, local spatial and temporal alkalinization in subapical regions might render ADF more active, resulting in increased actin polymerization and growth (Gungabissoon et al., 1998). However, unexpectedly, GFP-NtADF1 has been observed to colocalize with actin filament bundles in pollen tubes; overexpression of GFP-NtADF1 caused bundles or patches of F-actin and resulted in inhibited growth (Chen et al., 2002). It was proposed that local H^+ gradients in the pollen tube apex were likely to affect its actin-depolymerizing activity, contributing to actin remodeling, and that this regulation of the stability and organization of this ADF-rich actin mesh in elongating pollen tubes might play a role in regulating both growth rate and growth orientation. This was experimentally examined by altering the $[pH]_{cyt}$ of *L. formosanum* pollen tubes (Lovy-Wheeler et al., 2006); data suggested that intracellular pH might act as a regulator of oscillatory pollen tube growth by acting on ADF activity.

Here, we show large acidification of $[pH]_{cyt}$ in pollen tubes undergoing SI. Our observation that ADF decorates F-actin foci in SI-induced and artificially acidified pollen provides in vivo evidence that the actin-depolymerizing activity of ADF is altered by SI-induced $[pH]_{cyt}$ alterations. Our data are consistent with the idea that SI-induced acidification alters ADF activity, so that it has considerably reduced actin-depolymerizing activity and instead, decorates F-actin. This provides a good explanation for the extraordinary stability of these F-actin structures, which are resistant to 1 μM latrunculin B, whereas F-actin in growing pollen tubes is completely destroyed by this treatment (Poulter et al., 2010). Thus, in the context of SI, our data are consistent with the idea that ADF plays a pivotal role in the formation and stabilization of the SI-induced actin foci caused by acidified $[pH]_{cyt}$. The timing of this fits very nicely with the start of the major shift in pH measured at 30 and 60 min. We propose that this may play an important role in making SI irreversible. Exactly how F-actin aggregation is mediated to allow the formation of the distinctive SI-induced F-actin foci is currently not known. However, it is clear that ADF (perhaps in association with other ABPs) plays an important role in modulating this event through a pH-regulated alteration to its usual activity in growing pollen tubes.

The other ABP associated with the SI-induced punctate foci is CAP. CAP sequesters actin monomers, prevents them from polymerization in vitro, and also, promotes the severing of actin filaments in association with ADF (Barrero et al., 2002; Chaudhry et al., 2007; Deeks et al., 2007; Ono, 2013). Plant CAP is likely to be a key regulator of actin dynamics using a mechanism unique to plants (Staiger et al., 2010; Ono, 2013). The loss-of-function *cap1* mutant in Arabidopsis has major defects in pollen germination and tube growth, with altered actin configuration consistent with a major role for CAP in regulating actin dynamics (Deeks et al., 2007). Regarding a role for pH in regulating plant CAP activity, to our knowledge, there are no data. Animal ADF/cofilins efficiently sever actin filaments at basic pH but not neutral or acidic pHs (Yonezawa et al., 1985; Hawkins et al., 1993; Hayden et al., 1993). This might hint that, in SI-induced pollen, acidification might prevent CAP's actin severing activity. Confusingly, a recent study has shown that, in *Listeria monocytogenes*, CAP alone can sever actin filaments at an acidic pH but not a neutral pH, but together, CAP1 and ADF/cofilin promote severing of actin filaments within a wide pH range (Normoyle and Brieher, 2012). This seems to be an unlikely scenario in the pollen SI system, where we see both CAP and ADF associated with stable F-actin structures under conditions of low $[pH]_{cyt}$. This study suggests that CAP monomer binding and actin severing activity are reduced under acidic conditions. However, interestingly, in *L. monocytogenes*, it has recently been suggested that, at acidic pHs, CAP's actin severing factor may serve to produce filament ends that could seed actin assembly reactions (Normoyle and Brieher, 2012). This observation suggests a potential role for CAP under SI conditions: as the cytosol acidifies, CAP might be important in producing filament ends to seed actin assembly by ADF under acidic conditions. This will be something to test in the future.

We have shown here that shifting the $[pH]_{cyt}$ is both necessary and sufficient for triggering PCD. This has also been recently reported by Fendrych et al. (2014). Our finding that alterations in $[pH]_{cyt}$ also trigger alterations in actin, ADF, and CAP localization is unique and places these in a unique, biologically relevant scenario involving PCD in pollen. It is of interest that overexpression of wild-type CAP1 in several animal cells stimulated cofilin/ADF-induced apoptosis (Wang et al., 2008). Although it is relatively well established

that actin can act as both a sensor and a mediator of cell death, translating stress signals into alterations in actin polymerization status (Franklin-Tong and Gourlay, 2008; Desouza et al., 2012), relatively few studies have examined this in plant cells with respect to a mechanistic understanding. Moreover, the occurrence of F-actin foci has not been reported in many systems. They seem to be similar to Hirano bodies found in animal cells undergoing neurodegenerative diseases or cellular stresses, which are associated with ADF/cofilin (Bamburg and Wiggan, 2002). In Brewer's yeast (*Saccharomyces cerevisiae*), CAP (Srv2p in yeast) localizes to actin patches (Lila and Drubin, 1997) and is required for the formation of F-actin bodies (Gourlay et al., 2004) in stressed, quiescent Brewer's yeast (Sagot et al., 2006). Several plant systems have been observed to exhibit F-actin reorganization during PCD, and it is thought that the polymeric status of actin acts as a dynamic, integrated feedback mechanism for the health status of a cell, with PCD signaling major alterations (Smertenko and Franklin-Tong, 2011). Drawing comparisons with a study providing a link between actin alterations and signaling to apoptosis in lymphocytes (Hao and August, 2005), it has been suggested that a similar scenario may operate in plant cells and that alterations to the plant actin cytoskeleton could potentially signal directly to PCD (Tian et al., 2009). However, mechanistically, we have no idea of what might be involved. It would be of considerable interest to examine other plant systems undergoing PCD for alterations in $[pH]_{cyt}$, actin, ADF, and CAP organization to see if this is a more general phenomenon.

MATERIALS AND METHODS

Growth of Pollen Tubes and Treatments

Field poppy (*Papaver rhoeas*) pollen was hydrated and grown at 10 mg mL^{-1} in liquid germination medium [GM; 13.5% (w/v) Suc, 0.01% (w/v) H_3BO_3, 0.01% (w/v) KNO_3, and 0.01% (w/v) $Mg(NO_3)_2 0.6H_2O$] for at least 60 min before the addition of any treatments, which has been previously described in Snowman et al. (2002). For SI treatments, recombinant PrsS proteins were produced by cloning the nucleotide sequences specifying the mature peptide of the S_1, S_3, and S_8 alleles of the *S* gene (pPRS100, pPRS300, and pPRS800) into the expression vector pMS119 as described previously (Foote et al., 1994). Expression and purification of the proteins were performed as described by Foote et al. (1994). SI was induced by adding recombinant PrsS proteins (final concentration of 10 μg mL^{-1}) to pollen that had been grown for 1 h in vitro (Wilkins et al., 2011). Treatments with drugs involved the addition of the appropriate stock to the desired concentration; 50 mM propionic acid (pH 5.5 or 7.0) was used to manipulate cellular pH as stated in "Results." The calcium ionophore A23187 was used at 10 or 50 μM. Untreated controls had GM added instead of the treatment. Live-cell imaging of pollen tubes was carried out in 35-mm glass-bottom microwell culture dishes with a number 1.5 coverglass (MatTek Corp.) coated with 0.001% (w/v) poly-L-Lys.

Measurement of $[pH]_{cyt}$ of Pollen Tubes

Intracellular $[pH]_{cyt}$ was monitored in living pollen tubes with AM of the pH-sensitive fluorophore BCECF (Invitrogen) as described by Bosch and Franklin-Tong (2007). Pollen tubes were loaded with 1 μM BCECF for 3.5 min followed by a wash with GM. Pollen tubes were only imaged within 5 to 10 min after the addition of BCECF because this time frame allowed accurate reporting of $[pH]_{cyt}$. Samples could not be used after this 10-min period because of dye sequestration by organelle compartments. Images were taken sequentially using a Leica DM IRE2 Confocal Microscope under the following microscope settings: pH-dependent wavelength, excitation at 488 nm and 7% power; and pH-independent wavelength, excitation at 458 nm and 12% power. Emission was collected at 510 to 550 nm for both images. Using ImageJ software, a 50- × 50-pixel box was used to measure the mean intensity of the area of each pair of images (488 and 458 nm). A measurement was taken from each pollen tube image (488- and 458-nm images) at the same position on each image. Four pairs of measurements were collected for each tube. Each pair of measurements was used to create a ratio (pH-dependent:pH-independent ratio of 488:458 nm). The mean ratio values of each pollen tube were then used to determine the $[pH]_{cyt}$ of the pollen tube using a reference calibration curve with a pseudocytoplasm calibration set.

A calibration curve was carried out for each individual imaging session. In vitro calibration was performed using 40 μM BCECF-free acid (Invitrogen) in a pseudocytosol (100 mM KCl, 10 mM NaCl, 1 mM $MgSO_4$, 10 mM MES, and 10 mM HEPES adjusted to desired pH). Images were taken sequentially using the same microscope settings as those used for in vitro pollen tube measurements (488 and 458 nm). A pair of images was taken at each of the following pH values to create a calibration curve: pH 5.5, pH 6, pH 6.5, pH 7, pH 7.5, and pH 8. Using ImageJ software, intensities were measured for each pair of images, and a ratio value was calculated. These ratios were plotted to give a calibration curve to pH ratio, which was used to calculate the pH of individual pollen tubes after various treatments. Statistical analysis (Wilcoxon rank sum test) was carried out; where statistical comparisons are made, they are between samples at the same time point.

Visualization of F-Actin and ABPs in Field Poppy Pollen Tubes

Field poppy pollen tubes were fixed with 400 μM 3-maleimodobenzoic acid *N*-hydroxysuccunumide ester (Pierce; 10 mM stock in dimethyl sulfoxide) for 6 min at room temperature followed by 2% (w/v) formaldehyde freshly prepared from paraformaldehyde for 1 h at 4°C. Pollen was collected, and supernatant was removed. The pollen pellet was washed three times in 1× Tris-buffered saline (TBS; pH 7.6) and resuspended in 100 μL of TBS. Actin was stained using 66 nM rhodamine phalloidin, which only binds F-actin and not G-actin. The fixed pollen samples were incubated with rhodamine phalloidin overnight at 4°C. For quantification, pollen F-actin was assessed as described by Poulter et al. (2010). For each of seven independent experiments, 50 pollen tubes were scored for actin configuration for each treatment; 100 pollen tubes were scored for each treatment in another three experiments, and in total, 3,800 pollen tubes were scored per treatment. Statistical analysis was carried out using ANOVA. For ABP colocalization experiments, pollen tubes were stabilized, fixed, and subsequently, incubated in 0.05% (w/v) cellulose/0.05% (w/v) macerozyme with 0.1% (v/v) Triton X-100 in MES buffer containing 0.1 mM phenylmethylsulfonyl fluoride and 1% (w/v) bovine serum albumin for 15 min. Cells were washed in MES and then TBS, and they were incubated in 1% (w/v) bovine serum albumin in TBS for 30 min. Samples were incubated with either rabbit anti-AtCAP1 or rabbit anti-LlADF primary antibody at 1:500 at 4°C. After TBS washes, pollen was then incubated with the secondary antibody goat anti-rabbit IgG:fluorescein isothiocyanate (1:300; Sigma-Aldrich) and 66 nM rhodamine-phalloidin for 1.5 h. In total, 700 pollen tubes were scored for actin foci and ABP colocalization over three independent experiments. Colocalization of actin foci with the ABPs was assessed in overlaid confocal images by manually identifying the actin foci in a region of interest in the red channel and then, scoring for the presence or absence of the ABP in the region of interest in the green channel. Results are reported as percentages of pollen tubes with foci that colocalized with the ABP.

Caspase Activity Assays

Caspase-3-like/DEVDase activity in living, growing pollen tubes was visualized with the cell permeant ImageIT Live Caspase 3 & 7 Detection Kit (Invitrogen). Pregrown pollen was incubated with the 0.1× solution of FAM-DEVD-FMK FLICA regent in GM for 60 min. Pollen was subsequently washed in GM and imaged using an epifluorescence microscope using fluorescein isothiocyanate filters. The level of fluorescence in pollen tubes indicated the presence and level of caspase-3 and caspase-7 activity in the cell. Only pollen tubes scored as pollen grains display strong autofluorescence; 50 pollen tubes were scored for each treatment, and three independent replicates were performed. Student's *t* test was used for statistical analysis.

Pyrophosphatase Assays on Recombinant p26.1a and p26.1b at Different pHs

Activity assays for sPPase activity at different pH were performed using recombinant Pr-p26.1a and Pr-p26.1b proteins. The p26.1a and p26.1b constructs with an N-terminal His-Tag were transfected into *Escherichia coli* (BL21 strain), and expression was induced with 1 mM isopropylthio-β-galactoside and purified using Ni-agarose following the manufacturer's protocol (QIAGEN). To determine pyrophosphatase (sPPase) activity, a standard curve was constructed using different concentrations of NaH_2PO_4. For the assays, recombinant p261a and p261b were diluted to 10 μM into basic medium (50 mM HEPES KOH, pH 8.0, 50 μM EGTA, 2 mM $MgCl_2$ supplemented with 2 mM Mg^{++}, and 50 μM EGTA). To determine activity at different pHs, the buffer pH was adjusted before assaying. Fiske-Subbarow reagent was added to both standard curve solution and enzyme assay solution and left for 20 min at room temperature. The absorbance of each sample was read at optical density at 691 nm, and activities were calculated from the standard curve using known concentrations of NaH_2PO_4.

Vacuolar Labeling

Carboxy-DCFDA (Invitrogen) was used for vacuolar visualization. Pollen tubes were labeled with 1 μM carboxy-DCFDA (Invitrogen) for between 15 and 30 min and protected from light. Samples were washed in GM and imaged using a Leica DM IRE2 Confocal Microscope exciting with 488-nm lasers, and emission was collected with a 500- to 550-nm band-pass filter.

Standard recombinant DNA methodology was used to construct the vacuolar membrane marker δ-TIP-GFP used for transient expression in pollen tubes. The full-length δ-TIP coding sequence was amplified from the LAT52 promoter::GFP::δ-TIP construct (a gift from Natasha Raikhel) and cloned behind the pollen-specific promoter NTP303. GFP was expressed as a C-terminal fusion protein to yield NTP303::δ-TIP::GFP. Microprojectile bombardment was performed using the helium-driven PDS-1000/He Biolistic System (Bio-Rad) using tungsten particles (1.3 μm) coated with plasmid DNA. Images were acquired using confocal microscopy as previously described.

Supplemental Data

The following supplemental materials are available.

Supplemental Figure S1. Calibration of the $[pH]_{cyt}$ of field poppy pollen tube with the pH indicator BCECF AM.

Supplemental Figure S2. Cartoon showing a model of the integrated SI PCD signaling network in field poppy pollen.

Supplemental Figure S3. Ratiometric imaging of BCECF-labeled, SI-induced pollen tubes reveals cytosolic acidification.

Supplemental Figure S4. Acidification of the pollen tube cytosol triggers the formation of punctate F-actin foci and colocalization of CAP and ADF.

Supplemental Figure S5. Quantification of SI-induced alterations in vacuolar morphology.

Supplemental Figure S6. Artificial manipulation of $[pH]_{cyt}$ of pollen tube triggers alterations in vacuolar organization.

Supplemental Movie S1. Visualization of typical vacuolar movement in a field poppy pollen tube vacuole labeled with carboxy-DCFDA.

Supplemental Movie S2. Visualization of vacuolar alterations after SI in a field poppy pollen tube vacuole using δ-TIP-GFP.

ACKNOWLEDGMENTS

We thank Natasha Raikhel for providing the δ-TIP construct, Patrick Hussey for the LlADF antibody, and Chris Staiger for the CAP antibody.

Received October 28, 2014; accepted January 27, 2015; published January 28, 2015.

LITERATURE CITED

Allwood EG, Anthony RG, Smertenko AP, Reichelt S, Drobak BK, Doonan JH, Weeds AG, Hussey PJ (2002) Regulation of the pollen-specific actin-depolymerizing factor LlADF1. Plant Cell **14:** 2915–2927

Bamburg JR, McGough A, Ono S (1999) Putting a new twist on actin: ADF/cofilins modulate actin dynamics. Trends Cell Biol **9:** 364–370

Bamburg JR, Wiggan OP (2002) ADF/cofilin and actin dynamics in disease. Trends Cell Biol **12:** 598–605

Barrero RA, Umeda M, Yamamura S, Uchimiya H (2002) *Arabidopsis* CAP regulates the actin cytoskeleton necessary for plant cell elongation and division. Plant Cell **14:** 149–163

Bibikova TN, Jacob T, Dahse I, Gilroy S (1998) Localized changes in apoplastic and cytoplasmic pH are associated with root hair development in *Arabidopsis thaliana*. Development **125:** 2925–2934

Blatt MR, Armstrong F (1993) K^+ channels of stomatal guard-cells—abscisic-acid-evoked control of the outward rectifier mediated by cytoplasmic pH. Planta **191:** 330–341

Bosch M, Franklin-Tong VE (2007) Temporal and spatial activation of caspase-like enzymes induced by self-incompatibility in *Papaver* pollen. Proc Natl Acad Sci USA **104:** 18327–18332

Bosch M, Poulter NS, Vatovec S, Franklin-Tong VE (2008) Initiation of programmed cell death in self-incompatibility: role for cytoskeleton modifications and several caspase-like activities. Mol Plant **1:** 879–887

Bozhkov PV, Filonova LH, Suarez MF, Helmersson A, Smertenko AP, Zhivotovsky B, von Arnold S (2004) VEIDase is a principal caspase-like activity involved in plant programmed cell death and essential for embryonic pattern formation. Cell Death Differ **11:** 175–182

Carlier MF, Laurent V, Santolini J, Melki R, Didry D, Xia GX, Hong Y, Chua NH, Pantaloni D (1997) Actin depolymerizing factor (ADF/cofilin) enhances the rate of filament turnover: implication in actin-based motility. J Cell Biol **136:** 1307–1322

Chaudhry F, Guérin C, von Witsch M, Blanchoin L, Staiger CJ (2007) Identification of Arabidopsis cyclase-associated protein 1 as the first nucleotide exchange factor for plant actin. Mol Biol Cell **18:** 3002–3014

Chen CY, Wong EI, Vidali L, Estavillo A, Hepler PK, Wu HM, Cheung AY (2002) The regulation of actin organization by actin-depolymerizing factor in elongating pollen tubes. Plant Cell **14:** 2175–2190

Coffeen WC, Wolpert TJ (2004) Purification and characterization of serine proteases that exhibit caspase-like activity and are associated with programmed cell death in *Avena sativa*. Plant Cell **16:** 857–873

Danon A, Rotari VI, Gordon A, Mailhac N, Gallois P (2004) Ultraviolet-C overexposure induces programmed cell death in Arabidopsis, which is mediated by caspase-like activities and which can be suppressed by caspase inhibitors, p35 and Defender against Apoptotic Death. J Biol Chem **279:** 779–787

de Graaf BH, Rudd JJ, Wheeler MJ, Perry RM, Bell EM, Osman K, Franklin FC, Franklin-Tong VE (2006) Self-incompatibility in *Papaver* targets soluble inorganic pyrophosphatases in pollen. Nature **444:** 490–493

Deeks MJ, Rodrigues C, Dimmock S, Ketelaar T, Maciver SK, Malhó R, Hussey PJ (2007) Arabidopsis CAP1 - a key regulator of actin organisation and development. J Cell Sci **120:** 2609–2618

del Pozo O, Lam E (1998) Caspases and programmed cell death in the hypersensitive response of plants to pathogens. Curr Biol **8:** 1129–1132

Desouza M, Gunning PW, Stehn JR (2012) The actin cytoskeleton as a sensor and mediator of apoptosis. BioArchitecture **2:** 75–87

Fasano JM, Swanson SJ, Blancaflor EB, Dowd PE, Kao TH, Gilroy S (2001) Changes in root cap pH are required for the gravity response of the *Arabidopsis* root. Plant Cell **13:** 907–921

Feijó JA, Sainhas J, Hackett GR, Kunkel JG, Hepler PK (1999) Growing pollen tubes possess a constitutive alkaline band in the clear zone and a growth-dependent acidic tip. J Cell Biol **144:** 483–496

Feijó JA, Sainhas J, Holdaway-Clarke T, Cordeiro MS, Kunkel JG, Hepler PK (2001) Cellular oscillations and the regulation of growth: the pollen tube paradigm. BioEssays **23:** 86–94

Felle H, Brummer B, Bertl A, Parish RW (1986) Indole-3-acetic acid and fusicoccin cause cytosolic acidification of corn coleoptile cells. Proc Natl Acad Sci USA **83:** 8992–8995

Felle HH (2001) pH: signal and messenger in plant cells. Plant Biol **3:** 577–591

Felle HH, Kondorosi E, Kondorosi A, Schultze M (1998) The role of ion fluxes in Nod factor signalling in *Medicago sativa*. Plant J **13:** 455–463

Fendrych M, Van Hautegem T, Van Durme M, Olvera-Carrillo Y, Huysmans M, Karimi M, Lippens S, Guérin CJ, Krebs M, Schumacher K, et al (2014) Programmed cell death controlled by ANAC033/SOMBRERO determines root cap organ size in Arabidopsis. Curr Biol **24:** 931–940

Foote HCC, Ride JP, Franklin-Tong VE, Walker EA, Lawrence MJ, Franklin FCH (1994) Cloning and expression of a distinctive class of self-incompatibility (S) gene from Papaver rhoeas L. Proc Natl Acad Sci USA **91:** 2265–2269

Franklin-Tong N, Franklin C (1993) Gametophytic self-incompatibility: contrasting mechanisms for *Nicotiana* and *Papaver*. Trends Cell Biol **3:** 340–345

Franklin-Tong VE, Gourlay CW (2008) A role for actin in regulating apoptosis/programmed cell death: evidence spanning yeast, plants and animals. Biochem J **413:** 389–404

Franklin-Tong VE, Hackett G, Hepler PK (1997) Ratio-imaging of $Ca^{2+}{}_i$ in the self-incompatibility response in pollen tubes of *Papaver rhoeas*. Plant J **12:** 1375–1386

Franklin-Tong VE, Ride JP, Read ND, Trewavas AJ, Franklin FCH (1993) The self-incompatibility response in *Papaver rhoeas* is mediated by cytosolic-free calcium. Plant J **4:** 163–177

Fricker MD, White NS, Obermeyer G (1997) pH gradients are not associated with tip growth in pollen tubes of *Lilium longiflorum*. J Cell Sci **110:** 1729–1740

Fukuda H (2000) Programmed cell death of tracheary elements as a paradigm in plants. Plant Mol Biol **44:** 245–253

Gibbon BC, Kropf DL (1994) Cytosolic pH gradients associated with tip growth. Science **263:** 1419–1421

Gourlay CW, Carpp LN, Timpson P, Winder SJ, Ayscough KR (2004) A role for the actin cytoskeleton in cell death and aging in yeast. J Cell Biol **164:** 803–809

Gungabissoon RA, Jiang CJ, Drøbak BK, Maciver SK, Hussey PJ (1998) Interaction of maize actin-depolymerising factor with actin and phosphoinositides and its inhibition of plant phospholipase C. Plant J **16:** 689–696

Hao S, August A (2005) Actin depolymerization transduces the strength of B-cell receptor stimulation. Mol Biol Cell **16:** 2275–2284

Hara-Nishimura I, Hatsugai N (2011) The role of vacuole in plant cell death. Cell Death Differ **18:** 1298–1304

Hara-Nishimura I, Hatsugai N, Nakaune S, Kuroyanagi M, Nishimura M (2005) Vacuolar processing enzyme: an executor of plant cell death. Curr Opin Plant Biol **8:** 404–408

Hatsugai N, Kuroyanagi M, Yamada K, Meshi T, Tsuda S, Kondo M, Nishimura M, Hara-Nishimura I (2004) A plant vacuolar protease, VPE, mediates virus-induced hypersensitive cell death. Science **305:** 855–858

Hawkins M, Pope B, Maciver SK, Weeds AG (1993) Human actin depolymerizing factor mediates a pH-sensitive destruction of actin filaments. Biochemistry **32:** 9985–9993

Hayden SM, Miller PS, Brauweiler A, Bamburg JR (1993) Analysis of the interactions of actin depolymerizing factor with G- and F-actin. Biochemistry **32:** 9994–10004

Hicks GR, Rojo E, Hong S, Carter DG, Raikhel NV (2004) Germinating pollen has tubular vacuoles, displays highly dynamic vacuole biogenesis, and requires VACUOLESS1 for proper function. Plant Physiol **134:** 1227–1239

Higaki T, Goh T, Hayashi T, Kutsuna N, Kadota Y, Hasezawa S, Sano T, Kuchitsu K (2007) Elicitor-induced cytoskeletal rearrangement relates to vacuolar dynamics and execution of cell death: in vivo imaging of hypersensitive cell death in tobacco BY-2 cells. Plant Cell Physiol **48:** 1414–1425

Johannes E, Collings DA, Rink JC, Allen NS (2001) Cytoplasmic pH dynamics in maize pulvinal cells induced by gravity vector changes. Plant Physiol **127:** 119–130

Jones AM (2001) Programmed cell death in development and defense. Plant Physiol **125:** 94–97

Jones AM, Dangl JL (1996) Logjam at the Styx: programmed cell death in plants. Trends Plant Sci **1:** 114–119

Katsuhara M, Kuchitsu K, Takeshige K, Tazawa M (1989) Salt stress-induced cytoplasmic acidification and vacuolar alkalization in *Nitellopsis obtusa* cells: *in vivo* P-nuclear magnetic resonance study. Plant Physiol **90:** 1102–1107

Korthout HA, Berecki G, Bruin W, van Duijn B, Wang M (2000) The presence and subcellular localization of caspase 3-like proteinases in plant cells. FEBS Lett **475:** 139–144

Kuchitsu KY, Sakano K, Shibuya N (1997) Transient cytoplasmic pH change and ion fluxes through the plasma membrane in suspension-cultured rice cells triggered by N-Acetylchitooligosaccharide elicitor. Plant Cell Physiol **38:** 1012–1018

Kurkdjian A, Guern J (1989) Intracellular pH: measurement and importance in cell activity. Annu Rev Plant Physiol Plant Mol Biol **40:** 271–303

Li S, Samaj J, Franklin-Tong VE (2007) A mitogen-activated protein kinase signals to programmed cell death induced by self-incompatibility in *Papaver* pollen. Plant Physiol **145:** 236–245

Lila T, Drubin DG (1997) Evidence for physical and functional interactions among two *Saccharomyces cerevisiae* SH3 domain proteins, an adenylyl cyclase-associated protein and the actin cytoskeleton. Mol Biol Cell **8:** 367–385

Lovy-Wheeler A, Kunkel JG, Allwood EG, Hussey PJ, Hepler PK (2006) Oscillatory increases in alkalinity anticipate growth and may regulate actin dynamics in pollen tubes of lily. Plant Cell **18:** 2182–2193

Maciver SK, Hussey PJ (2002) The ADF/cofilin family: actin-remodeling proteins. Genome Biol **3:** reviews3007

Mathieu Y, Lapous D, Thomine S, Laurière C, Guern J (1996) Cytoplasmic acidification as an early phosphorylation-dependent response of tobacco cells to elicitors. Planta **199:** 416–424

Messerli MA, Robinson KR (1998) Cytoplasmic acidification and current influx follow growth pulses of *Lilium longiflorum* pollen tubes. Plant J **16:** 87–91

Morley SC, Sun GP, Bierer BE (2003) Inhibition of actin polymerization enhances commitment to and execution of apoptosis induced by withdrawal of trophic support. J Cell Biochem **88:** 1066–1076

Normoyle KP, Brieher WM (2012) Cyclase-associated protein (CAP) acts directly on F-actin to accelerate cofilin-mediated actin severing across the range of physiological pH. J Biol Chem **287:** 35722–35732

Obara K, Kuriyama H, Fukuda H (2001) Direct evidence of active and rapid nuclear degradation triggered by vacuole rupture during programmed cell death in *Zinnia*. Plant Physiol **125:** 615–626

Ono S (2013) The role of cyclase-associated protein in regulating actin filament dynamics - more than a monomer-sequestration factor. J Cell Sci **126:** 3249–3258

Parton RM, Fischer S, Malhó R, Papasouliotis O, Jelitto TC, Leonard T, Read ND (1997) Pronounced cytoplasmic pH gradients are not required for tip growth in plant and fungal cells. J Cell Sci **110:** 1187–1198

Poulter NS, Bosch M, Franklin-Tong VE (2011) Proteins implicated in mediating self-incompatibility-induced alterations to the actin cytoskeleton of *Papaver* pollen. Ann Bot (Lond) **108:** 659–675

Poulter NS, Staiger CJ, Rappoport JZ, Franklin-Tong VE (2010) Actin-binding proteins implicated in the formation of the punctate actin foci stimulated by the self-incompatibility response in *Papaver*. Plant Physiol **152:** 1274–1283

Poulter NS, Vatovec S, Franklin-Tong VE (2008) Microtubules are a target for self-incompatibility signaling in *Papaver* pollen. Plant Physiol **146:** 1358–1367

Rojo E, Martín R, Carter C, Zouhar J, Pan S, Plotnikova J, Jin H, Paneque M, Sánchez-Serrano JJ, Baker B, et al (2004) VPEgamma exhibits a caspase-like activity that contributes to defense against pathogens. Curr Biol **14:** 1897–1906

Roos W, Evers S, Hieke M, Tschope M, Schumann B (1998) Shifts of intracellular pH distribution as a part of the signal mechanism leading to the elicitation of benzophenanthridine alkaloids: phytoalexin biosynthesis in cultured cells of *eschscholtzia californica*. Plant Physiol **118:** 349–364

Rotari VI, He R, Gallois P (2005) Death by proteases in plants: whodunit. Physiol Plant **123:** 376–385

Rudd JJ, Franklin F, Lord JM, Franklin-Tong VE (1996) Increased phosphorylation of a 26-kD pollen protein is induced by the self-incompatibility response in Papaver rhoeas. Plant Cell **8:** 713–724

Rudd JJ, Franklin-Tong VE (1999) Calcium signaling in plants. Cell Mol Life Sci **55:** 214–232

Rudd JJ, Franklin-Tong VE (2003) Signals and targets of the self-incompatibility response in pollen of *Papaver rhoeas*. J Exp Bot **54:** 141–148

Rudd JJ, Osman K, Franklin FCH, Franklin-Tong VE (2003) Activation of a putative MAP kinase in pollen is stimulated by the self-incompatibility (SI) response. FEBS Lett **547:** 223–227

Sagot I, Pinson B, Salin B, Daignan-Fornier B (2006) Actin bodies in yeast quiescent cells: an immediately available actin reserve? Mol Biol Cell **17:** 4645–4655

Sanmartín M, Jaroszewski L, Raikhel NV, Rojo E (2005) Caspases: regulating death since the origin of life. Plant Physiol **137:** 841–847

Scott AC, Allen NS (1999) Changes in cytosolic pH within Arabidopsis root columella cells play a key role in the early signaling pathway for root gravitropism. Plant Physiol **121:** 1291–1298

Shen J, Zeng Y, Zhuang X, Sun L, Yao X, Pimpl P, Jiang L (2013) Organelle pH in the Arabidopsis endomembrane system. Mol Plant **6:** 1419–1437

Smertenko A, Franklin-Tong VE (2011) Organisation and regulation of the cytoskeleton in plant programmed cell death. Cell Death Differ **18:** 1263–1270

Snowman BN, Kovar DR, Shevchenko G, Franklin-Tong VE, Staiger CJ (2002) Signal-mediated depolymerization of actin in pollen during the self-incompatibility response. Plant Cell **14:** 2613–2626

Staiger CJ, Poulter NS, Henty JL, Franklin-Tong VE, Blanchoin L (2010) Regulation of actin dynamics by actin-binding proteins in pollen. J Exp Bot **61:** 1969–1986

Thomas SG, Franklin-Tong VE (2004) Self-incompatibility triggers programmed cell death in *Papaver* pollen. Nature **429:** 305–309

Thomas SG, Huang S, Li S, Staiger CJ, Franklin-Tong VE (2006) Actin depolymerization is sufficient to induce programmed cell death in self-incompatible pollen. J Cell Biol **174:** 221–229

Tian M, Chaudhry F, Ruzicka DR, Meagher RB, Staiger CJ, Day B (2009) Arabidopsis actin-depolymerizing factor AtADF4 mediates defense signal transduction triggered by the *Pseudomonas syringae* effector *AvrPphB*. Plant Physiol **150:** 815–824

van Doorn WG (2011) Classes of programmed cell death in plants, compared to those in animals. J Exp Bot **62:** 4749–4761

van Doorn WG, Beers EP, Dangl JL, Franklin-Tong VE, Gallois P, Hara-Nishimura I, Jones AM, Kawai-Yamada M, Lam E, Mundy J, et al (2011) Morphological classification of plant cell deaths. Cell Death Differ **18:** 1241–1246

van Doorn WG, Woltering EJ (2005) Many ways to exit? Cell death categories in plants. Trends Plant Sci **10:** 117–122

Wang C, Zhou GL, Vedantam S, Li P, Field J (2008) Mitochondrial shuttling of CAP1 promotes actin- and cofilin-dependent apoptosis. J Cell Sci **121:** 2913–2920

Wheeler MJ, Vatovec S, Franklin-Tong VE (2010) The pollen S-determinant in Papaver: comparisons with known plant receptors and protein ligand partners. J Exp Bot **61:** 2015–2025

Wilkins KA, Bancroft J, Bosch M, Ings J, Smirnoff N, Franklin-Tong VE (2011) Reactive oxygen species and nitric oxide mediate actin reorganization and programmed cell death in the self-incompatibility response of *papaver*. Plant Physiol **156:** 404–416

Wilkins KA, Poulter NS, Franklin-Tong VE (2014) Taking one for the team: self-recognition and cell suicide in pollen. J Exp Bot **65:** 1331–1342

Wu J, Wang S, Gu Y, Zhang S, Publicover SJ, Franklin-Tong VE (2011) Self-incompatibility in *Papaver rhoeas* activates nonspecific cation conductance permeable to Ca^{2+} and K^+. Plant Physiol **155:** 963–973

Yonezawa N, Nishida E, Sakai H (1985) pH control of actin polymerization by cofilin. J Biol Chem **260:** 14410–14412

Young B, Wightman R, Blanvillain R, Purcel SB, Gallois P (2010) pH-sensitivity of YFP provides an intracellular indicator of programmed cell death. Plant Methods **6:** 27–36

Wilkins et al.
Supplemental Figure 1. Calibration of the cytosolic pH of *Papaver* pollen tube with the pH indicator BCECF AM

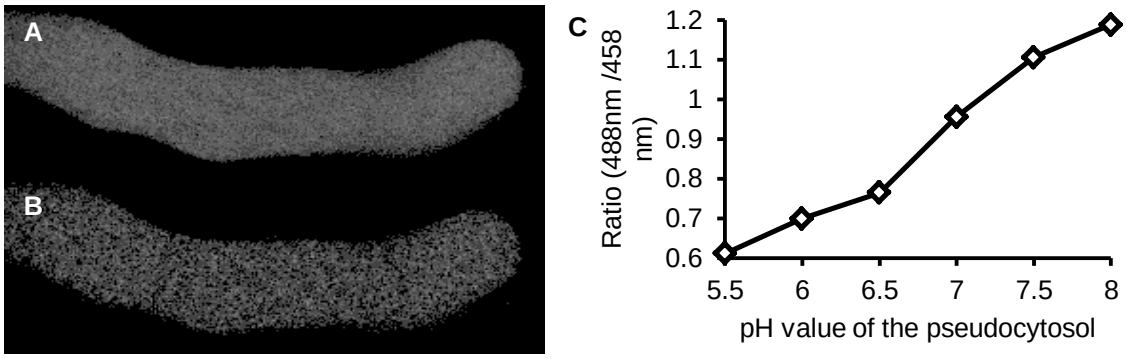

Wilkins et al. Supplemental Figure 1. Calibration of the cytosolic pH of *Papaver* pollen tube with the pH indicator BCECF AM

A healthy, growing pollen tube was labelled with the pH indicator BCECF-AM prior to ratiometric imaging using confocal microscopy. A ratio value was made of the two images using Image J; this ratio was used to determine the pH of the pollen tube cytosol using a calibration curve (**C**), collected during the same experiment. This pollen tube has a cytosolic pH of 6.8.

(**A**) BCECF-AM signal when excited at 488 nm, emission at 510-550 nm. (**B**) BCECF-AM signal when excited at 458 nm, emission at 510-550 nm. (**C**) Pseudocytosol solutions of between pH 5-8, at approximately 0.5 intervals, were labelled with BCECF free acid and sequential confocal images were collected (excitation 488nm, then 458nm, emission 510-550 nm). A ratio of the two images was calculated and plotted as ratio: pH values.

Wilkins et al.

Supplemental Fig. 2. Cartoon showing a model of the integrated self-incompatibility (SI) programmed cell death (PCD) signalling network in *Papaver rhoeas* pollen.

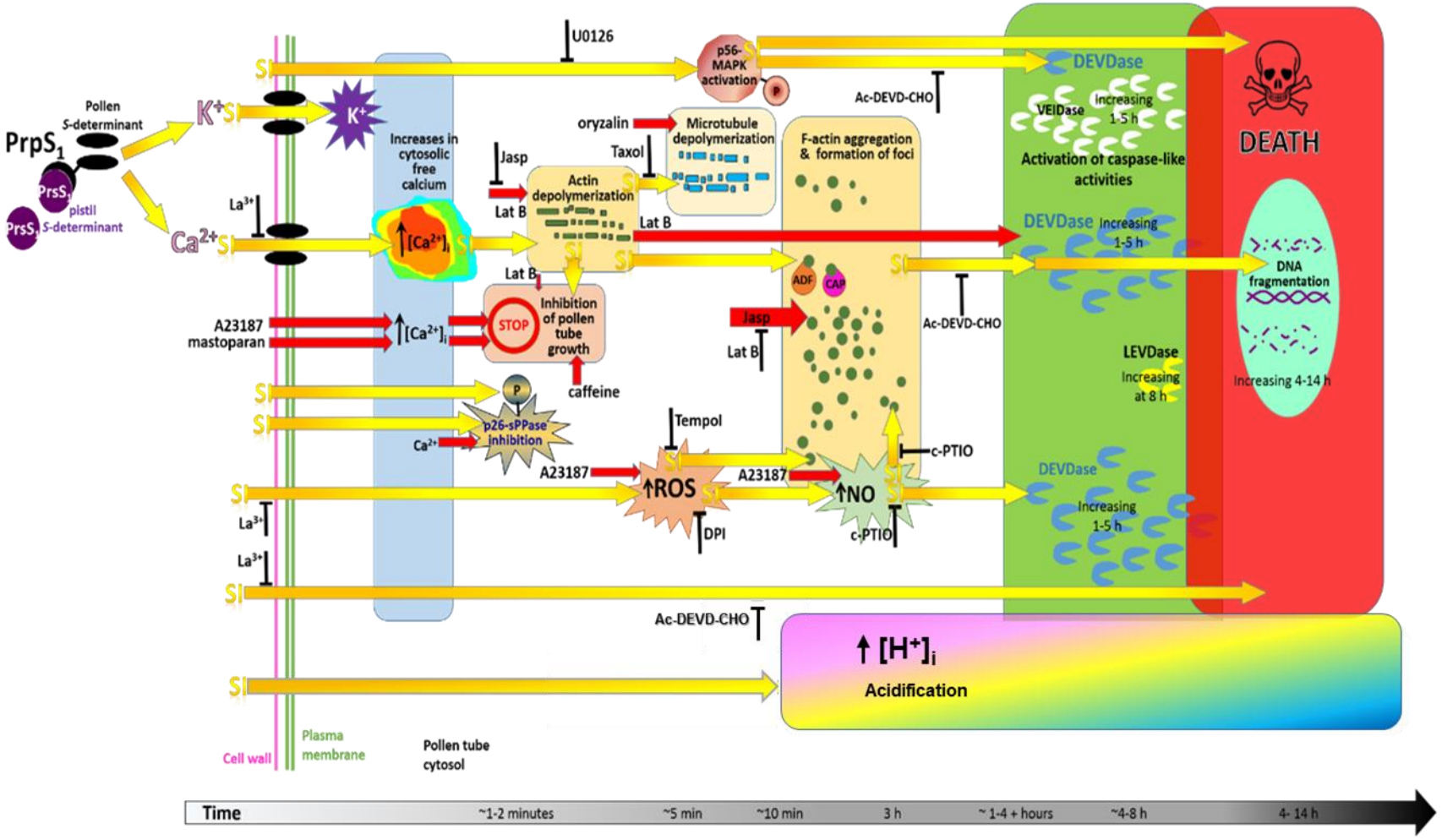

Legend: Supplemental Fig. 2. Cartoon showing a model of the relative timing and integration of the components identified in the self-incompatibility (SI) programmed cell death (PCD) signaling network in *Papaver rhoeas* pollen.

Interaction of a pistil *S*-determinant PrsS with its cognate pollen *S*-determinant, PrpS, in a *S* haplotype-specific manner (e.g. PrsS1 with PrpS1) rapidly triggers the SI signalling network, resulting in the rapid inhibition of pollen tube tip growth and culminating with DNA fragmentation and death of incompatible pollen. Different colored boxes indicate key events triggered by SI; grey arrow indicates approximate timings; yellow arrows show SI-induced events; red arrows indicate agonist drugs used to stimulate events; black symbols show drugs used to inhibit events; pink vertical line represents the cell wall; double green line represents the plasma membrane.

One of the earliest events include rapid influx of Ca^{2+} and K^{+}, and almost instantaneous increases in cytosolic free Ca^{2+} ($[Ca^{2+}]_{cyt}$; blue box). $[Ca^{2+}]_{cyt}$ increases are required for many SI events, including phosphorylation and inactivation of soluble inorganic pyrophosphatases (sPPases) Pr-26.1a/b, actin depolymerization, and transient increases in reactive oxygen species (ROS) and nitric oxide (NO). Moreover, mastoparan or the Ca^{2+} ionophore A23187 (red arrows) can mimic SI-induced increases in) $[Ca^{2+}]_{cyt}$. Lanthanum (La^{3+}) has been used extensively to block SI-induced Ca^{2+} events and has demonstrated a requirement for Ca^{2+} as a key mediator of SI signaling to death. This places $[Ca^{2+}]_{cyt}$ signaling as one of the first SI events, upstream of many of the targets.

The end focus of the SI-induced network appears to be DNA fragmentation and cell death (red box), which are inhibited by pretreatment with the tetrapeptide inhibitor Ac-DEVD-CHO, but not Ac-YVAD-CHO. The inferred DEVDase activity has been more directly measured using the tetrapeptide substrate, Ac-DEVD-AMC, which is cleaved by SI-induced pollen extracts. This approach revealed three activities (green box): DEVDase and VEIDase increase between 1–5 h post SI and LEVDase increases later (still increasing at 8 h). DEVDase activity peaks at 5 h and has been shown to be required for DNA fragmentation, which can be prevented by the DEVDase inhibitor Ac-DEVD-CHO. These activities are optimal at pH 5. The caspase-like activities, which do not have any activity at normal cytosolic pH, need the pollen cytosol to acidify. We previously showed this occured in the first few hours of SI; here we have shown it begins at ~10 min and stablizes at ~pH 5.5 at 60 min (rainbow box).

Several components appear to be integrated in signaling to SI-mediated cell death. Central to this is the cytoskeleton (yellow boxes). SI-stimulates actin depolymerization, which causes inhibition of pollen tube growth. Low concentrations of Latrunculin B (Lat B) also inhibits pollen tube tip growth (orange box). SI triggers much higher levels of depolymerization than that required to inhibit pollen tube growth and higher concentrations of LatB that mimic this triggers activation of a DEVDase activity (measured with the Ac-DEVD-AMC substrate) and DNA fragmentation that is prevented by pretreatment with Ac-DEVD-CHO and not Ac-YVAD-CHO. Moreover, low concentrations of actin stabilizing Jasplakinolide (Jasp) can counteract and alleviate SI- or Lat B-induced DNA fragmentation, presumably by lowering the level of actin depolymerization. Subsequently, in SI, F-actin aggregates form highly stable punctate F-actin foci that are resistant to depolymerization and are associated with the actin-binding proteins (ABPs) actin-depolymerizing factor (ADF), and cyclase-associated protein (CAP; yellow box). High concentrations of Jasp can also trigger DNA fragmentation which is alleviated by pretreatment with Ac-DEVD-CHO and not Ac-YVADCHO. The formation of stable F-actin foci may be analogous to the stabilization using Jasp. Caffeine, which inhibits pollen tube growth without affecting the cytoskeleton, does not trigger DNA fragmentation. Together, these data implicate actin dynamics in modulating the DEVDase activity. SI also triggers microtubule depolymerization. This can be mimicked by use of the microtubule depolymerizer, oryzalin. Actin depolymerization using LatB triggers microtubule depolymerization but not vice versa, suggesting that SI-induced F-actin depolymerization signals to microtubule depolymerization. The tubulin-stabilizing drug, taxol, alleviates SI-induced Ac-DEVDAMC cleavage, implicating a requirement for tubulin depolymerization for the DEVDase activation. Disrupting microtubule dynamics alone using oryzalin does not trigger increased cleavage of the DEVDase substrate Ac-DEVD-AMC: this suggests that both actin and microtubule depolymerization are required for DEVDase-mediated SI-induced PCD. Evidence for involvement of a SI-activated p56-MAPK comes from use of the MEK inhibitor U0126 and its negative analogue U0124. Although U0126 inhibits pollen tube growth and p56-MAPK activity, it does not affect pollen viability. These drugs provided evidence that p56-MAPK activation is required for the activation of a DEVDase, DNA fragmentation, and cell death. SI stimulates transient increases in ROS and later NO. Pretreatment of pollen tubes with either the NADPH oxidase inhibitor diphenyliodonium or the NO scavenger cPTIO and then stimulating SI showed that both were required to reduce the SI-induced DEVDase activity. This suggests that ROS and NO act in concert or tandem to signal to activate SI-induced PCD through the activation of a DEVDase activity. Moreover, these drugs alleviated the formation of the characteristic punctate F-actin foci. This implicates ROS and NO signaling for the formation of these F-actin foci.

From: ***K.A. Wilkins et al. (2014). Taking one for the team: self-recognition and cell suicide in pollen.*** J. Exp. Bot. (2014) 65 (5): 1331-1342 doi:10.1093/jxb/ert468

Supplemental Figure 3. Ratiometric-imaging of BCECF-labelled SI-induced pollen tubes reveal cytosolic acidification

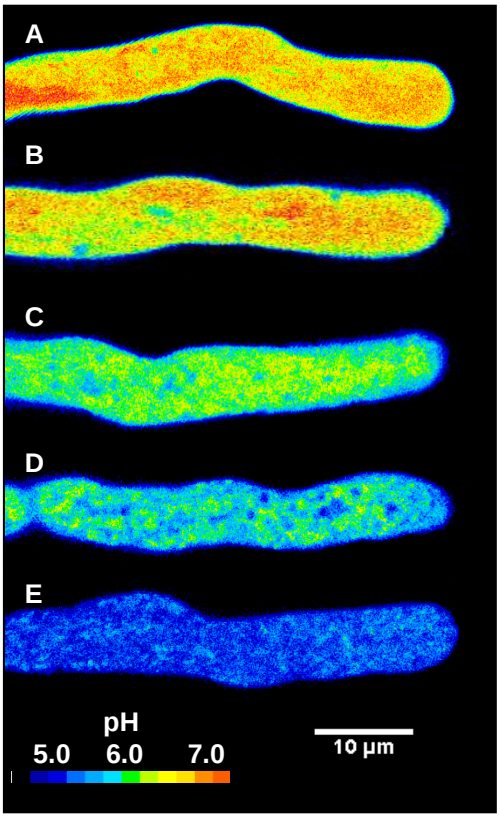

Supplemental Figure 3. Ratiometric-imaging of BCECF-labelled SI-induced pollen tubes reveal cytosolic acidification

(**A-E**) Representative ratiometric images of pollen tube cytosol using the pH indicator BCECF AM (488 nm excitation and 510-550 emission) after background subtraction.

(**A**) Untreated pollen tube cytosol at T=0, pH 7.1. (**B**) Untreated pollen tube cytosol at T=60, pH 7.15. (**C**) SI-induced pollen tube cytosol 10 min after addition of PrsS, pH 6.4. (**D**) SI-induced pollen tube 30 min after addition of PrsS, pH 6.1. (**E**) SI-induced pollen tube 60 min after addition of PrsS, pH 5.5. Calibration of the cytosolic pH is indicated by the inset colour scale. Scale bar 10 µm.

Wilkins et al. **Supplemental Figure 4. Acidification of the pollen tube cytosol triggers the formation of punctate F-actin foci and co-localization of CAP and ADF**

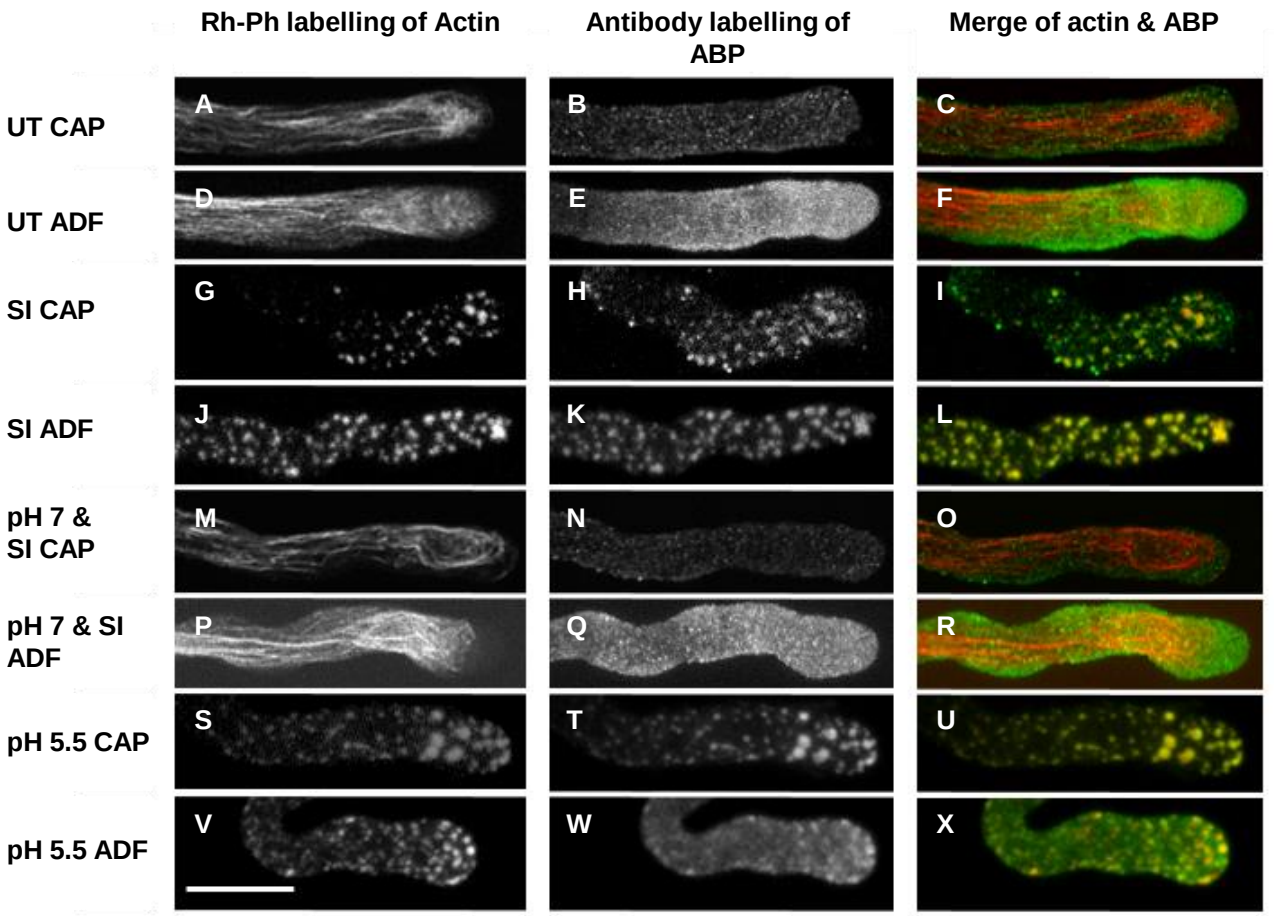

Supplemental Figure 4. Acidification of the pollen tube cytosol triggers the formation of punctate F-actin foci and co-localization of CAP and ADF

Representative images of untreated pollen tubes showing Rhodamine-Phalliodin (Rh-Ph) labelling of actin (first column), immunolocalized with either rabbit anti-AtCAP1 (CAP; cyclase-associated protein) or rabbit anti-LlADF (ADF; actin-depolymerizing factor) antibodies (second column), and merged images of Rh-Ph (red) and antibody labelling (green) (third column), following 3 h treatment with growth medium (UT), SI, propionic acid pH 5.5, propionic acid pH 7 & SI.

(**A**) Untreated F-actin, (**B**) Untreated CAP, (**C**) Merge of (**A**) and (**B**). (**D**) Untreated F-actin, (**E**) Untreated ADF, (**F**) Merge of (**D**) and (**E**). (**G**) SI F-actin, (**H**) SI CAP, (**I**) Merge of (**G**) and (**H**). (**J**) SI F-actin, (**K**) SI ADF, (**L**) Merge of (**J**) and (**K**). (**M**) pH 7 and SI F-actin, (**N**) pH 7 and SI CAP, (**O**) Merge of (**M**) and (**N**). (**P**) pH 7 and SI F-actin, (**Q**) pH 7 and SI ADF, (**R**) Merge of (**P**) and (**Q**). (**S**) pH 5.5 F-actin, (**T**) pH 5.5 CAP, (**U**) Merge of (**S**) and (**T**). (**V**) pH 5.5 F-actin, (**W**) pH 5.5 ADF, (**X**) Merge of (**V**) and (**W**). Scale bar = 10 µm.

Wilkins et al.
Supplemental Figure 5. Quantification of SI-induced alterations in vacuolar morphology

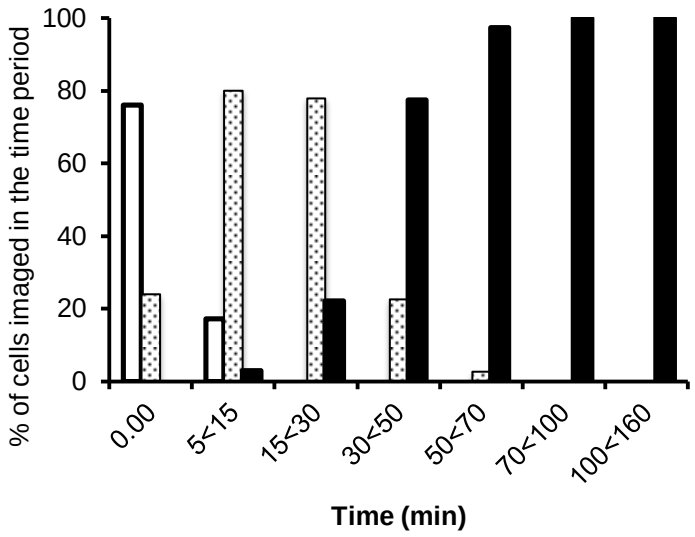

Supplemental Figure 5. Quantification of SI-induced alterations in vacuolar morphology

Pollen was labelled with the vacuolar marker c-DCFDA and the SI response was induced by the addition of PrsS. Pollen tubes were then assigned to one of three categories referring to vacuolar morphology. These categories includes (**i**) clear reticulate vacuolar network, white bars, (**ii**) reorganization, dotted bars, and (**iii**) extensive breakdown with no distinct network, black bars. N=214.

Wilkins et al. **Supplemental Figure 6. Artificial manipulation of cytosolic pH of pollen tube triggers alterations in vacuolar organization.**

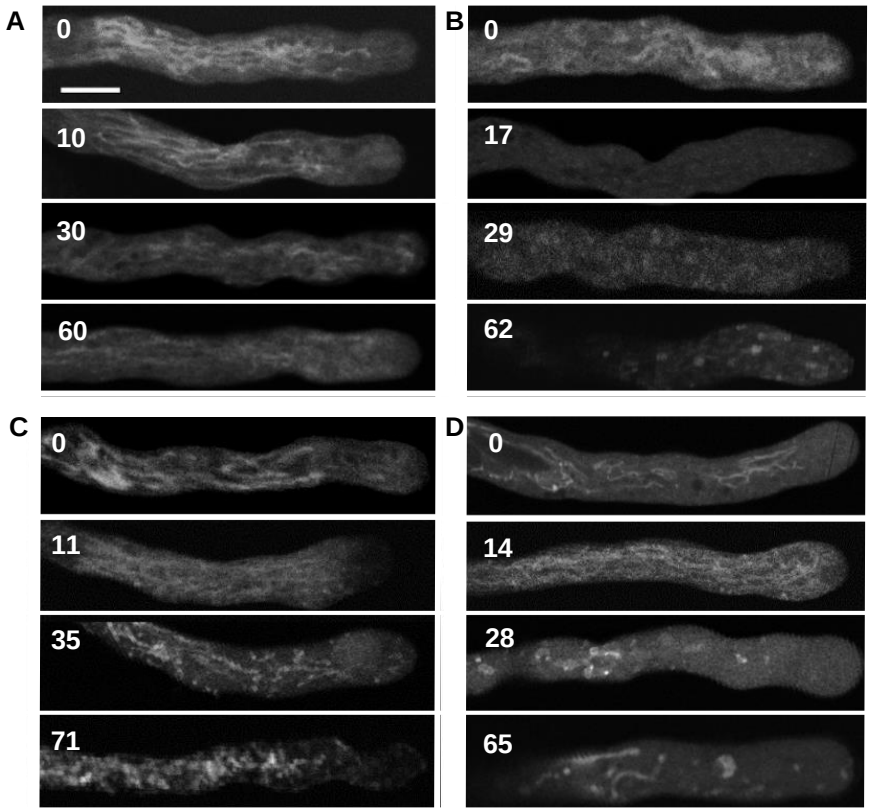

Supplemental Figure 6. Artificial manipulation of cytosolic pH of pollen tube triggers alterations in vacuolar organization

Papaver pollen tubes were: (**A**) untreated (incubated in growth medium) or treated with (**B**) 50 mM propionic acid pH 5.5 to mimic SI-induced acidification, (**C**) pre-treated with 50 mM propionic acid pH 7 for 10 min prior to addition of PrsS, or (**D**) 50 mM propionic acid pH 7. The vacuole was then labelled with c-DCFDA. Scale bar, 10 µm.

(**A**) The vacuole of untreated pollen tubes at 0, 10, 30, and 60 minutes did not undergo any reorganization or disruption of the vacuole. (**B**) Pollen tubes treated with propionic acid pH 5.5, underwent vacuole reorganization within 17 min, with no tubular structure visible. By 62 min only small spots of vacuolar signal remained. This provides evidence that acidification of the cytosol has an extreme effect on the organization and the stability of the vacuole in *Papaver* pollen tubes, and suggests that acidification of the cytosol may play a role in triggering vacuolar breakdown. (**C**) SI-induced pollen pre-treated with propionic acid pH 7 for 10 minutes underwent some reorganization within the first 11 min and the typical reticulate structure was not as well defined. At 35 min the vacuole underwent major reorganization and aggregated into bundles. Further aggregation continued thereafter, and at 71 min of treatment there were only pockets of vacuolar signal remaining, indicating that it had not completely broken down. Blocking SI-induced acidification with propionic acid pH 7 results in vacuolar reorganization but not vacuolar breakdown. (**D**) Pollen tubes treated with propionic acid pH 7 showed slight reorganization of the vacuolar signal at 14 min; the typical reticulate structure was not so well defined and had moved into the pollen tube tip. The vacuole continued to reorganize into tight bundles of vacuolar signal, but did not appear to undergo vacuolar breakdown.